Russian Geology and Geophysics © 2020, V.S. Sobolev IGM, Siberian Branch of the RAS
Vol. 61, No. 12, pp. 1354–1373, 2020 *DOI:10.15372/RGG2020149* *Geologiya i Geofizika*

The Role of Black-Shale Strata in the Formation of the Natalka and Pavlik Gold Deposits (Yana–Kolyma Orogenic Belt)

T.I. Mikhalitsyna[a,b,] ✉, O.T. Sotskaya[a]

[a]*N.A. Shilo Northeastern Interdisciplinary Scientific Research Institute, Far Eastern Branch of the Russian Academy of Sciences, ul. Portovaya 16, Magadan, 685000, Russia*

[b]*Northeastern State University, ul. Portovaya 13, Magadan, 685000, Russia*

Received 27 July 2018; received in revised form 12 March 2020; accepted 7 May 2020

Abstract—Data on geochemistry, distribution of ore and rare-earth elements and precious metals, and micromineralogy are presented. The objects of study are late Permian sedimentary and volcanosedimentary deposits of the Tikhonya Brook (Atkan (P_3at) and Omchak (P_3om) formations) and hydrothermally metamorphosed rocks of the Natalka and Pavlik gold deposits of the Omchak ore–placer cluster. Analysis of the deposit ores showed enrichment in chalcophile trace elements Au, Ag, As, W, and Sb relative to their average contents in the upper crust and the host Permian rocks. The high contents of W and Bi in the ores suggest the participation of a magmatic fluid. The absence of abnormal contents of Ni, Co, Sb, Mo, Cr, and Se indicates the redeposition of these elements from ore-bearing rocks, without their input by ore-forming fluids, which is confirmed by the isotopic composition of sulfide sulfur and the characteristics of carbonaceous ore material. The formation of deposits proceeded with a change in REE contents. All objects show similar trace-element patterns: The rocks are enriched in LREE and lack a Ce anomaly. The identical REE patterns of ores reflect their inheritance from unaltered late Permian deposits. It has been established that the ores formed under different redox conditions, mainly with the participation of a relatively oxidized fluid enriched in LREE of the hydrothermal system NaCl–H_2O, with domination of Cl over F. The studies have shown that the host carbonaceous sedimentary complexes, which served as additional sources of precious and associated metals, played a crucial role in the formation of the Natalka and Pavlik gold deposits. Some of the ore elements in the unaltered deposits form their own minerals.

Keywords: Late Permian; black-shale strata; Natalka and Pavlik gold deposits; rare-earth elements (REE); ore minerals; precious metals; microinclusions; micromineralogy

INTRODUCTION

Permian deposits are widespread within the Kular–Nera turbidite terrane, which is part of the Yana–Kolyma orogenic belt. They host the large Natalka, Pavlik, and Degdekan gold deposits located in northeastern Asia and a number of precious-metal ore occurrences of different sizes. The high interest of researchers to Permian deposits is primarily due to different views of the source of metals and ore formation and to the particular role of ore-bearing strata in the formation of gold mineralization. Formation of gold deposits localized in carbonaceous-terrigenous (black shale) complexes is usually interpreted in the framework of models of sedimentary (Gar'kovets, 1973; Button, 1976), hydrothermal-sedimentary (Hutchinson, 1987; Konstantinov et al., 1988; Konstantinov, 1993), volcanosedimentary (Barnett et al., 1982; Tomich, 1986), and metamorphogenic (Boyle, 1979; Buryak, 1982; Buryak et al., 1988) ore formation. One of the main drawbacks of such models is their insufficient support by special lithological and geochemical studies of ore-bearing carbonaceous-terrigenous complexes. Since these deposits are poor in gold, the high gold contents of ore-bearing areas might be due to a subcrustal source of ore elements. Such elements are supplied with submarine hydrothermal solutions during terrigenous sedimentation. The metamorphogenic model does not explain the low contents of gold in rocks subjected to metamorphism. The contents of gold supplied from sedimentary strata are insufficient for the formation of its deposits (Konstantinov, 1993; Safonov, 1997).

Studies of the gold contents of carbonaceous-terrigenous complexes in northeastern Asia (Sidorov and Volkov, 1998, 2001, 2002; Sidorov and Thomson, 2000) showed that zones of sulfide-disseminated mineralization in black-shale strata, called basic formations, can be an intermediate source of gold during the formation of endogenous deposits. The degree of lithogenesis and the specifics of authigenic mineral formation depend significantly on the facies composition of sediments and the geodynamic type of evolution of sedimentary basins (Yapaskurt, 1999). At the same time, it was shown that the phase differentiation of matter, induced by hypergenesis and sediment genesis, continues during dia-

✉ Corresponding author.
E-mail address: tim_66@mail.ru (T.I. Mikhalitsyna)

genesis and catagenesis and, depending on the tectonic setting, leads to the formation of stratiform deposits of copper, lead, zinc, or uranium (Kholodov, 1982, 2001; Kholodov and Shmariovich, 1992).

Thus, ore-forming processes in sedimentary strata are intimately related to the specifics of lithogenesis and the degree of postsedimentary transformations, which, in turn, depend on the geodynamic setting. Taking into account all these facts, it is necessary to consider the prehistory of the formation of gold deposits in carbonaceous-terrigenous complexes within the framework of ore-lithogenic systems. As for the ore-bearing terrigenous strata of the Yana–Kolyma orogenic belt, there are a number of insufficiently studied issues, namely, the behavior of gold during various geologic processes, the role of the host rocks, their lithologic and geochemical characteristics, and the regularities of the localization of gold mineralization in the certain lithologic and stratigraphic units of sediments.

Therefore, we chose objects that made it possible to obtain a new factual material on the chemical composition of variably altered rocks, using modern research methods.

The study area is located within the Ayan–Yuryakh anticlinorium, which is one of the largest tectonic structures of the terrane. It borders upon the In'yali–Debin synclinorium in the northeast and is part of the Yana–Kolyma metallogenic belt. A specific feature of the area is domination of gold–quartz ores (forming numerous placer deposits) over other types of ore mineralization (Khanchuk, 2006).

The Ayan–Yuryakh anticlinorium is a linearly folded structure with gentle flanks complicated by high-rank folds, with a predominance of NW-striking faults, and with E–W-striking faults hosting dikes and granitoid plutons. It is formed by mainly Permian marine terrigenous and volcanoterrigenous deposits subdivided into the Pioner ($P_{1\text{-}2}$pn), Atkan (P_3at), Omchak (P_3om), and Staratel' (P_3st) formations (Biakov and Vedernikov, 1990) (Fig. 1). The sedimentary unit is intruded by granitoid bodies and dikes of different compositions and ages (J_3–K_1). Within the study area, the sedimentary rocks were transformed by initial regional greenschist facies metamorphism, as evidenced by the hosted low-temperature mineral assemblages.

FACTUAL MATERIAL AND METHODS OF STUDY

This research is based on the materials obtained by us during the field work and studies in the Laboratory of Petrology, Isotope Geochronology and Ore Formation of the Northeastern Interdisciplinary Scientific Research Institute, Magadan.

Rock material was sampled from natural exposures in the southwest (Tikhonya Brook on the right bank of the Nel'koba River, remote from large faults and ore objects; 107 samples) and at the center (Omchak ore–placer cluster; 99 samples) of the Ayan–Yuryakh anticlinorium. The main criterion for sampling was the presence of unoxidized iron sulfides and no obvious hypergene alteration of rocks. A total of 43 samples of unaltered rocks and 46 rock samples from gold deposits were analyzed.

The starting sample material was rock fragments 5–10 to 10–15 cm in size. The samples were crushed in a mortar to obtain a heavy fraction for micromineralogical studies, which prevented contamination of the samples at this stage.

The micromineralogical composition of rocks was determined by scanning electron microscopy with electron probe microanalysis (EPMA). The contents of major oxides and trace elements in the rocks were determined by X-ray fluorescence and atomic-emission spectral analyses (Analytical Center of the Northeastern Interdisciplinary Scientific Research Institute, Magadan). The contents of precious and rare-earth elements were determined by mass spectrometry with inductively coupled plasma (ICP MS) (Common Use Center of the Institute of Tectonics and Geophysics, Khabarovsk).

The main problem in the study of disseminated gold–sulfide ores is their significant dispersion, which complicates their reliable analysis by common mineralogical methods. Therefore, along with the classical methods of petrographic (Axioplan Imaging polarizing microscope), mineralogical, and geochemical analyses, we used highly sensitive and precise methods of special electron microscope study of ores.

Micromineralogical studies were carried out on a QEMSCAN automated system (Australia, Germany). It is an EVO-50 scanning electron microscope equipped with four Bruker energy-dispersive spectrometers (EDS) and a Quantax X-ray microanalysis system. The device has EDS detectors located opposite each other, which permits an analysis of unpolished samples.

The search for mineral inclusions and their study were performed in the back-scattered electrons (BSE) mode, when the brightness of a phase correlates with its mean atomic number. Precious metals having a large atomic number exhibit a bright "glow" as compared with other minerals.

The minerals of the heavy fraction of ores were studied after their separation in bromoform. Then, samples of two types were prepared: (1) the minerals were applied as a thin layer on a carbonaceous tape and sprayed with carbon; (2) the minerals were mounted in polished epoxy-resin blocks. Operating conditions: accelerating voltage 25 kV, beam current 120 pA, emission region ~4 μm across, and magnification >500. During the analyses of fine phases (smaller than the X-ray generation zone or commensurate with it), the matrix matter was captured. Therefore, it was necessary to remove the matrix elements and recalculate the resulted bulk chemical composition. These recalculations were based on the data obtained by a microscope study of the thin sections. All electron microscope images are presented in the BSE mode.

To reconstruct the original nature of metasedimentary rocks, we considered their REE patterns, because REE show inert behavior at the early stages of metamorphism (Balashov, 1976; Efremova and Stafeev, 1985; Kholodov, 2001). The mobility of lanthanides is still a debatable issue. As follows from the literature data (Grauch, 1989; Lottermoser,

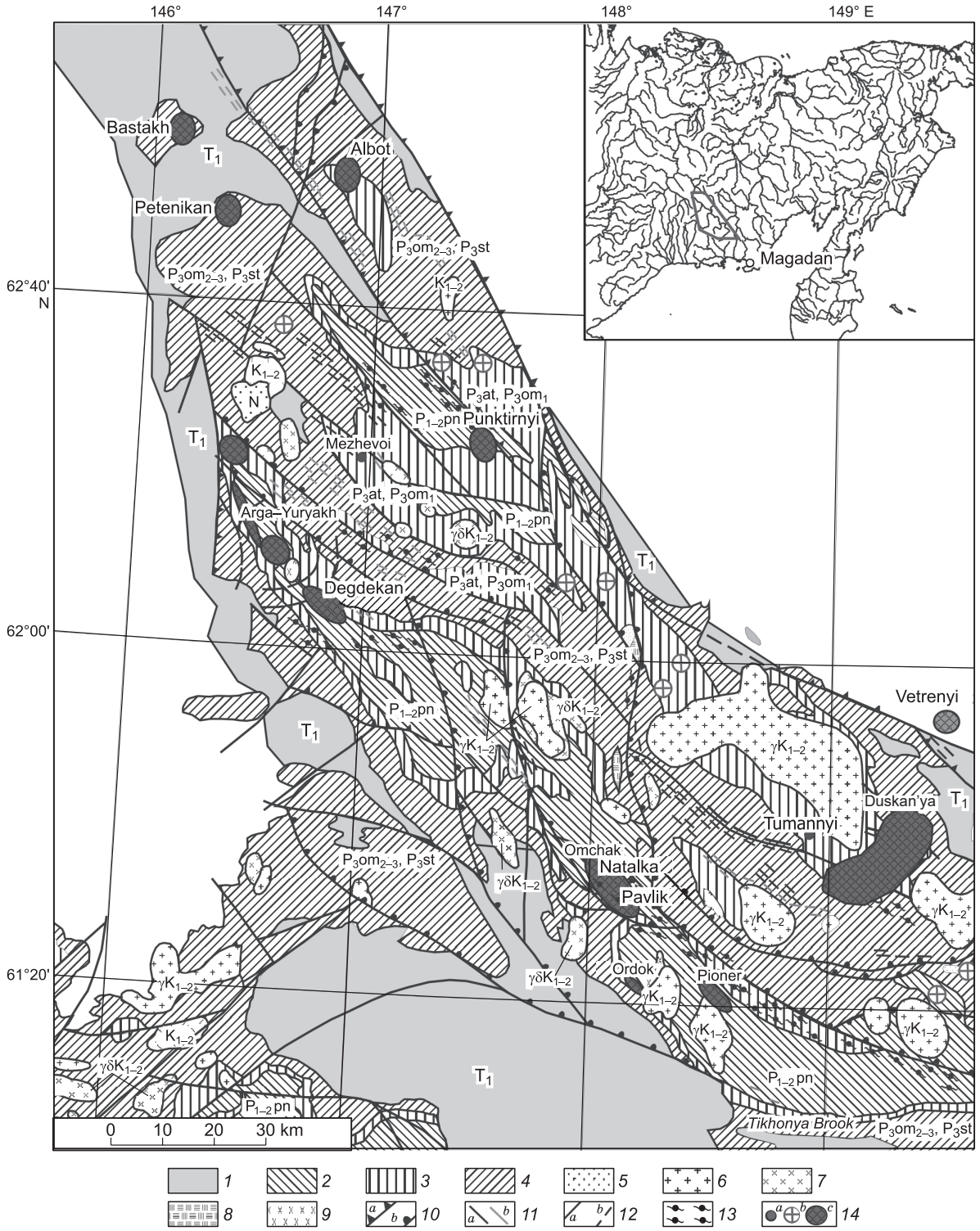

Fig. 1. Schematic geologic structure of the Ayan–Yuryakh anticlinorium (Astakhov et al., 2010). *1–5*, sediments: *1*, T_1, undivided; *2*, $P_{1–2}$pn; *3*, P_3at, P_3om_1; *4*, $P_3om_{2–3}$, P_3st; *5*, N; *6*, $\gamma K_{1–2}$ granites, granite-porphyry, and leucogranites; *7*, $\gamma\delta K_{1–2}$ granodiorites and granodiorite-porphyry; *8*, λK_2 subvolcanic rhyolites and rhyodacites; *9*, $\delta K_{1–2}$ diorites; *10*, reverse faults (*a*), thrusts (*b*); *11*, dikes: λJ_3 (*a*), $q\mu J_3$ (*b*); *12*, faults: proved (*a*), predicted (*b*); *13*, regional metamorphosed greenschist facies rocks; *14*, ore occurrences (*a*), ore clusters with mineralization sites and placers (*b*), ore clusters with deposits and ore occurrences (*c*).

1992), REE are the most mobile in hydrothermal and metasomatic processes (Kolonin et al., 2001), less mobile during low- and moderate-temperature metamorphism (Hellman et al., 1979; Ague, 2001), and are inert during high-temperature metamorphism (Muecke et al., 1979; Gil'bert et al., 1988; Bingen et al., 1996).

Rare-earth elements were studied in the late Permian sedimentary and volcanosedimentary rocks (Atkan and Omchak formations) of the Tikhonya Brook and in the metasomatic and ore-bearing rocks of the Natalka and Pavlik gold deposits. The REE patterns were chondrite-normalized (Taylor and McLennan, 1985). The REE compositions were estimated from the following parameters: $Eu_{an} = Eu/Eu^* = Eu_N/(Sm_N \times Gd_N)^{1/2}$; $Ce_N = Ce/Ce^* = Ce_N/((2La_N + Sm_N)/3)$ (Dubinin, 2006). To compare the chemical composition of ore-bearing and unaltered rocks, we considered the following petrochemical parameters: normalized alkalinity index (NAI) — $(Na_2O + K_2O)/Al_2O_3$, alkali index (AI) — Na_2O/K_2O, femic index (FI) — $(Fe_2O_3 + FeO + MnO + MgO)/SiO_2$, hydrolysate index (HI) — $(TiO_2 + Al_2O_3 + Fe_2O_3 + FeO + MnO)/SiO_2$, and potassium index (PI) — K_2O/Al_2O_3 (Yudovich and Ketris, 2000).

OUTLINE OF THE OBJECTS OF STUDY

The objects of study are the Natalka and Pavlik primary gold deposits discovered by an ore-prospecting team guided by E.P. Mashko in 1942. As a reference object for studying the chemical composition of the main ore-bearing strata, we chose a section made up of late Permian monoclinal rocks, from the deposits of the Atkan Formation (P_3at) to the Lower Triassic deposits (T_1), more than 4000 m in total thickness. It is located along the Tikhonya Brook (right bank of the Nel'koba River) on the southwestern flank of the Ayan–Yuryakh anticlinorium, within the northeastern limb of the Ten'ka anticline, at a distance from ore objects (Fig. 1) (Mikhalitsyna, 2011, 2014). Below, we briefly describe the lithology of two late Permian formations (from bottom to top) hosting the Natalka and Pavlik gold deposits.

The Atkan Formation is a marking regional horizon owing to the specific structure. It is made up of massive or obscure-bedded sedimentary and volcanosedimentary rocks (diamictites). The clastics are predominantly effusive rocks; their amount varies from single grains "suspended" in the diamictite matrix to 50% or more (Mikhalitsyna, 2014). The presence of tuffs and the numerous *in situ* volcanic fragments and acute-angled glass fragments in the matrix point to sedimentation within the neighboring Okhotsk–Taigonos volcanic arc. This is also evidenced by Bhatia's diagrams for these volcanics, showing a REE distribution typical of an ensimatic island arc (Isbell et al., 2016). The U–Pb (SHRIMP) zircon dating of tuff interbeds in the diamictites yielded ages of 262.5 ± 0.2 and 269.8 ± 0.1 Ma, which is consistent with the fossils preserved in the matrix (Biakov et al., 2010; Davydov et al., 2016; Isbell et al., 2016).

By chemical composition, the deposits of the Atkan Formation are of sodium alkalinity (AI = 1.54). There is a direct correlation between the titanium and femic indices, which is due to the presence of effusive-rock inclusions (Table 1).

Table 1. Average chemical composition of the unaltered rocks and ore-bearing strata, wt.%

Component/index	PAAS	Unaltered rocks		Deposits	
				Natalka (P_3at)	Pavlik (P_3om)
		P_3at	P_3om	Average	Average
	20*	12	31	24	22
SiO_2	62.8	65.23	64.97	74.37	67.25
TiO_2	1.0	0.80	0.76	0.45	0.54
Al_2O_3	18.9	15.90	15.78	8.93	12.85
$Fe_2O_{3\,tot}$	6.5	6.08	5.21	3.15	4.40
MnO	0.11	0.10	0.05	0.08	0.11
MgO	2.2	2.08	1.60	1.36	1.43
CaO	1.3	0.59	0.86	2.57	2.38
Na_2O	1.2	3.49	3.05	2.60	1.62
K_2O	3.7	2.26	3.04	2.01	2.89
P_2O_5	0.16	0.14	0.23	0.10	0.13
HI	0.42	0.35	0.33	0.19	0.28
FI	0.14	0.12	0.10	0.07	0.09
TI	0.053	0.050	0.048	0.049	0.042
KI	0.20	0.14	0.19	0.22	0.22
NAI	0.26	0.36	0.39	0.54	0.35
AI	0.32	1.54	1.00	1.96	0.66

Note. Chemical analysis was carried out at the Analytical Center of the Northeastern Interdisciplinary Scientific Research Institute, Magadan (analyst S.V. Mikhailova). Hereafter, PAAS is the Post-Archean Australian Shale.
* Hereafter, number of samples.

The Omchak Formation is made up of alternating flyschoid sandstones, siltstones, and mudstones and has horizontal and, to a lesser extent, cross and gradational bedding. The contents of Na and K are unevenly distributed in the rocks. The coarse-grained rocks are characterized by $Na_2O/K_2O = 3.10$, $(Na_2O + K_2O)/(Al_2O_3) = 0.55$, $TiO_2/Al_2O_3 \leq 0.066$, and average AI = 1.00, and the clayey rocks, by $Na_2O/K_2O = 0.43–0.90$ and $TiO_2/Al_2O_3 = 0.035–0.041$.

In general, the late Permian rocks are of normal alkalinity, with domination of Na over K. Potassium alkalinity is specific to silt interbeds in the upper part of the Omchak Formation. The average content of organic carbon (C_{org}) is 0.45% in the Atkan Formation (P_3at) and 0.35% in the Omchak Formation (P_3om) (Vedernikov, 2009). As shown earlier (Kokin et al., 1999), the initial content of C_{org} in the sediments is twice as high as that in lithified rock, which gives grounds to regard the late Permian deposits under study as black-shale strata. There are single beds with C_{org} contents an order of magnitude higher than the background one (23%), but they were ignored during the calculation of the average C_{org} content (Vedernikov, 2009).

The rocks of both formations contain pyrite, rutile, and apatite. The lower beds of the Omchak Formation are the most enriched in pyrite. In the Atkan Formation, pyritization is observed in members of alternating diamictites and finely foliated mudstones. The total amount of pyrite is 1–3%, seldom reaching 30%. It comprises primary globular pyrite and metagenetic crystalline pyrite (Buryak et al., 2002). Study of the sulfur isotope composition of syngenetic pyrite showed its heterogeneity, $\delta^{14}S$ = +17.8 to –15.69‰, in contrast to vein pyrite having a stable light sulfur isotope (Chanyshev and Stepanov, 1987; Mirzekhanov and Mirzekhanova, 1991).

The content of gold in pyrite varies from 0.14 to 3 ppm (on average, 0.57 ppm), and in arsenopyrite it averages 1.34 ppm. In the late Permian rocks of the Ayan–Yuryakh anticlinorium, the average gold content in pyrite is 0.58 ppm (Chanyshev and Stepanov, 1987). Pyrrhotite occurs as scattered dissemination and small lenses in rocks; less often, it forms veins of two generations: magnetic and nonmagnetic. It is usually younger than pyrite.

Other sulfides (galena, sphalerite, and chalcopyrite) form fine dissemination and, less often, metacrystals (arsenopyrite) in the rock matrix, amounting to no more than 1–2%.

According to the intensity of chemical weathering in the provenance area, the deposits are classified as clayey rocks and graywackes (HI = 0.35 (P_3at) and 0.33 (P_3om)) and are normally alkaline (NAI = 0.36 (P_3at) and 0.39 (P_3om)) (Table 1).

The contents of trace elements Au, Ag, Co, Cu, Zn, Mo, Pb, and Bi and platinum group elements in the Permian rocks are higher or close to their clarke contents in the upper crust (Taylor and McLennan, 1985) (Table 2). We have identified typical geochemical associations: Mo–Pb–Li–Fe–Zn–Ag (1) and Mn–Cr–Ca–Co–Mg (2) in P_3at; Ca–Mn (1), Co–Ag–Cu (2), and Sn–Fe–Ni–Cr–Mg–Zn (3) in P_3om (Mikhalitsyna, 2014). According to the ICP MS data, the Au contents in the siltstones of the Omchak Formation are close to those in the diamictites of the Atkan Formation (Table 2). Platinum group elements are unevenly distributed throughout the section. The maximum Pd contents are found in the P_3om mudstones. The P_3at rocks have high Pt contents. The Permian rocks of the section show a strong Au–Pd correlation and a weak Au–Pt one.

The Natalka and Pavlik gold deposits. These gold deposits are part of the Omchak ore–placer cluster, which includes a large number of ore occurrences, mineralization sites, and placers. Mineralization is controlled by large faults of NW strike localized in the Ten'ka deep-fault zone. The terrigenous rocks of the Permian Verkhoyansk Complex in the study area are intruded by granite and granodiorite plutons and small bodies of different compositions. Among the igneous rocks, there are Early–Late Cretaceous volcanism relics (Goryachev, 2003) responsible for the late gold mineralization of the deposits (Sidorov et al., 2003).

The Natalka and Pavlik gold deposits are of the same metallogenic type. They are characterized by gold–quartz low-sulfide mineralization of the pyrite–arsenopyrite type and are localized in the zone of the chlorite–sericite subfacies of the greenschist metamorphism facies.

The Natalka deposit is one of the largest gold deposits in Russia. The Permian hydrothermally metamorphosed sedimentary and volcanosedimentary deposits of the Pioner (P_{1-2}pn), Atkan (P_3at), and Omchak (P_3om) formations are ore-bearing. The orebody location is controlled by lithology and stratigraphy. Most of the deposit orebodies are localized in the diamictites of the Atkan Formation. In the over- and underlying rocks, orebodies are traceable along large-fault zones for 200 m from their contact with the Atkan Formation (Struzhkov et al., 2006). The mineralization zone of the Natalka gold deposit extends for ~5 km, reaching 1 km in total width and 900–1000 m in vertical span. The gold mineralization is controlled by NW-striking faults and is predominantly of vein–veinlet type. The orebodies are zones of contiguous quartz veinlets with sites of metasomatic silicification and scarce quartz lenses and veins.

The deposit comprises more than 70 vein and ore minerals, with quartz prevailing (70–80%). Carbonates and feldspars are subordinate. The major ore minerals (95–99%) are arsenopyrite and pyrite; the accessory minerals are pyrrhotite, galena, sphalerite, scheelite, chalcopyrite, native gold, ilmenite, and rutile. Sulfides amount to ≤1–3 or, seldom, 5% (Goncharov et al., 2002).

The rock metasomatism is expressed as carbonation (pre-ore stage), beresitization (gold ore stage), and wallrock alteration with the formation of carbonate–feldspar–arsenopyrite–quartz veinlets. Carbonation is pronounced as replacement of chlorite and quartz by carbonates and weak sulfidization (the presence of pyrite or, less often, pyrrhotite) in the deposits of both formations (P_3at and P_3om). Hydrothermal alteration is manifested as beresitization, evidenced from the uniform dissemination of pyrite and the replacement of albite by sericite and quartz, and as the pres-

Table 2. Trace elements in the sedimentary and volcanosedimentary rocks of the Tikhonya Brook and in the ores of the Natalka and Pavlik gold deposits, ppm

Element	Composition of upper continental crust	Atkan Formation (P_3at)			Omchak Formation (P_3om)				Natalka deposit					Pavlik deposit				
		Average	Silty mudstone	Diamictite	Average	Mudstone	Siltstone	Sandstone	Average	Group				Average	Group			
										I	II	III	IV		I	II	III	IV
		7*	1	6	16	4	9	3	24	6	7	9	2	22	12	7	2	1
Co	10	15.50	16.79	15.31	12.39	12.78	12.23	12.27	5.98	7.15	10.01	2.91	2.16	6.52	6.43	8.51	2.49	1.77
Ni	20	8.42	15.14	7.46	9.86	8.94	9.91	10.98	12.51	18.30	17.31	7.22	2.18	12.76	12.83	14.47	5.02	15.52
Cu	25	22.21	19.57	22.59	22.15	20.13	22.61	23.61	11.28	17.80	17.55	4.03	2.42	23.66	33.56	15.85	3.42	0.001
Zn	71	90.11	104.26	88.09	127.51	86.98	90.27	88.12	44.79	64.06	65.91	24.52	0.75	71.85	78.90	87.24	11.62	0.09
As	1.5	15.71	7.11	14.48	8.3	3.81	10.24	11.59	53.08	16.03	31.57	88.69	79.21	2179.8	217.99	5548.35	2498.22	1505.6
Se	—	—	—	—	—	—	—	—	0.50	0.001	0.03	0.80	2.29	0.33	0.01	0.59	0.94	1.02
Te	—	—	—	—	—	—	—	—	0.73	0.001	0.001	1.11	3.74	0.001	0.001	0.001	0.001	0.001
Rb	112	60.54	90.07	54.64	95.61	78.67	102.14	98.63	52.43	89.23	68.21	25.93	6.01	84.03	98.04	84.15	37.73	7.69
Sr	350	78.44	47.76	84.57	115.95	168.00	107.57	74.67	198.03	346.57	226.79	111.99	38.91	210.97	248.80	195.10	99.08	91.96
Y	22	8.69	10.27	8.70	22.53	19.97	24.73	19.31	5.39	9.63	6.31	2.83	1.02	9.79	10.97	10.25	5.05	1.88
Zr	190	46.75	60.29	44.04	131.89	67.21	158.82	137.32	25.18	51.59	22.95	13.43	5.62	64.52	73.90	65.59	29.15	15.18
Nb	25	5.94	8.15	5.50	12.04	7.41	13.49	13.89	1.33	3.02	1.19	0.57	0.22	4.51	4.84	5.32	1.72	0.55
Mo	1.5	0.51	0.78	0.45	1.47	1.21	1.64	1.34	1.43	2.78	1.25	0.76	1.08	0.78	0.75	0.80	0.86	0.82
Sn	5.5	2.14	3.32	1.90	3.91	1.30	5.62	2.27	2.54	3.09	4.41	1.28	0.001	1.48	1.40	1.00	2.25	4.26
Sb	0.2	N.d.	N.d.	N.d.	N.d.	N.d.	N.d.	N.d.	1.12	0.63	0.93	1.59	1.11	3.22	2.80	4.09	3.70	1.24
W	2	0.69	0.89	0.65	1.35	0.80	1.75	0.86	16.57	46.32	5.86	8.06	3.11	7.25	4.74	1.37	9.02	4.86
Pb	20	9.34	10.33	9.14	36.19	13.37	50.07	24.95	17.45	37.57	9.54	13.27	3.60	18.33	20.81	20.06	3.49	6.13
Bi	0.127	1.83	1.12	1.93	2.71	1.12	3.46	2.84	0.09	0.19	0.09	0.05	0.03	4.37	0.33	13.16	0.06	0.07
La	30	11.65	18.38	10.30	30.37	20.52	34.06	32.44	11.36	19.90	13.05	6.27	2.73	28.05	31.71	30.01	10.75	5.03
Th	10.7	2.51	5.51	1.91	8.05	4.08	9.46	9.13	0.26	4.46	2.14	1.28	0.53	7.77	9.05	7.75	2.45	1.60
U	2.8	0.74	1.06	0.67	1.62	0.79	2.00	1.61	0.42	0.85	0.37	0.24	0.10	1.21	1.40	1.23	0.43	0.33
Ag	0.05	0.29	0.34	0.28	0.44	0.35	0.50	0.39	1.43	1.67	1.54	0.79	0.001	0.99	1.06	0.81	0.50	2.44
Au	$1.8 \cdot 10^{-3}$	0.03	0.07	0.02	0.01	$8.5 \cdot 10^{-4}$	0.02	$8.7 \cdot 10^{-3}$	4.34	9.94	0.39	4.44	0.94	0.72	0.66	0.53	0.18	3.86
Pt	N.d.	0.01	0.02	0.01	$2.1 \cdot 10^{-3}$	0.00	$2.8 \cdot 10^{-3}$	$2.8 \cdot 10^{-3}$	0.009	0.008	0.004	0.016	0.002	$1 \cdot 10^{-2}$	$7 \cdot 10^{-3}$	$2 \cdot 10^{-2}$	$5 \cdot 10^{-2}$	$9 \cdot 10^{-4}$
Pd	$5 \cdot 10^{-3}$	0.03	0.1	0.02	0.15	0.35	$3.0 \cdot 10^{-5}$	0.01	0.006	0.002	0.014	0.004	0.00	$7 \cdot 10^{-3}$	$1 \cdot 10^{-2}$	$4 \cdot 10^{-3}$	$7 \cdot 10^{-4}$	0.000
Ir	$2 \cdot 10^{-5}$	$1.4 \cdot 10^{-4}$	0.00	$1.6 \cdot 10^{-4}$	$8.0 \cdot 10^{-3}$	0.00	0.00	$3.0 \cdot 10^{-5}$	$1.3 \cdot 10^{-4}$	$4.0 \cdot 10^{-5}$	$3.9 \cdot 10^{-4}$	0.00	0.00	$4 \cdot 10^{-4}$	$6 \cdot 10^{-4}$	0.00	$1 \cdot 10^{-4}$	0.000
Ru	N.d.	$2.4 \cdot 10^{-4}$	0.00	$2.9 \cdot 10^{-4}$	$4.9 \cdot 10^{-5}$	0.00	$5.0 \cdot 10^{-6}$	$1.7 \cdot 10^{-4}$	$7.3 \cdot 10^{-4}$	$6.3 \cdot 10^{-4}$	$1.3 \cdot 10^{-3}$	$4.0 \cdot 10^{-4}$	$4.4 \cdot 10^{-4}$	$3 \cdot 10^{-4}$	$3 \cdot 10^{-4}$	$3 \cdot 10^{-4}$	$1 \cdot 10^{-4}$	$4 \cdot 10^{-4}$
Rh	N.d.	$6.1 \cdot 10^{-3}$	0.01	$5.2 \cdot 10^{-3}$	$1.5 \cdot 10^{-4}$	0.00	$3.8 \cdot 10^{-6}$	$5.7 \cdot 10^{-4}$	$6.0 \cdot 10^{-5}$	$1.0 \cdot 10^{-5}$	$1.6 \cdot 10^{-4}$	$2.0 \cdot 10^{-5}$	0.00	$1 \cdot 10^{-3}$	$1 \cdot 10^{-4}$	$4 \cdot 10^{-5}$	$1 \cdot 10^{-4}$	0.000
Co/Ni	0.50	1.99	1.11	2.11	1.33	1.50	1.31	1.17	0.76	0.45	0.57	1.00	1.23	0.56	0.58	0.59	0.51	0.11
U/Th	0.25	0.27	0.19	0.29	0.20	0.20	0.20	0.18	0.19	0.19	0.17	0.19	0.18	0.16	0.16	0.16	0.17	0.20
Th/La	0.35	0.19	0.30	0.17	0.25	0.19	0.27	0.28	0.20	0.22	0.16	0.20	0.19	0.28	0.30	0.27	0.23	0.32
Nb/La	0.83	0.50	0.44	0.52	0.40	0.37	0.40	0.43	0.11	0.15	0.09	0.09	0.09	0.16	0.16	0.18	0.16	0.11

Note. N.d., not detected; dash, no analyses. The composition of the upper continental crust is given after Taylor and McLennan (1985). The analyses were carried out by ICP MS at the Institute of Tectonics and Geophysics, Khabarovsk.

ence of quartz–feldspar, quartz–carbonate, and quartz veinlets with arsenopyrite inclusions. The maximum number of newly formed minerals is observed in the diamictites of the Atkan Formation (Alpatov and Mikhalitsyna, 2000).

The host rocks are characterized by high alkalinity (NAI = 0.54), with domination of sodium over potassium (Na_2O/K_2O (AI) = 1.96). In the intense-beresitization zone, the relative content of potassium increases (AI = 0.21). According to the hydrolysate index, the rocks are classified as clay-siliceous shales (HI = 0.19) (Table 1).

The rocks of the ore-bearing strata of the Natalka gold deposit have a varying content of carbonaceous matter (CM). Most of CM is localized as clusters of dispersed organic matter along the foliation zone. There are also finest (thousandths of mm to 0.1–0.2 mm) graphite flakes, isometric rounded, lenticular-oval, and angular inclusions of oil series CM (0.1–0.4 mm), and clusters of globular CM in small quartz and quartz–chlorite lenses (0.05–0.06 mm) (Pluteshko et al., 1988). The average carbon isotope composition ($\delta^{13}C$) of the rocks and ores of the Natalka deposit is about –22‰, and that of the tectonites is –17‰, which indicates the primary sedimentary nature of organic matter and the formation of carbonates in the rocks, tectonites, and ores through its transformation (Voroshin et al., 2000; Goncharov et al., 2002).

The Pavlik deposit is localized in the late Permian deposits of the Omchak and Atkan formations. The ore-controlling structures of the deposit are similar to those of the Natalka ore field. The deposit orebodies are confined to the feathering fractures of major faults, mostly to the shear fractures of NW strike. The rock metasomatism is expressed as beresitization (stockwork carbonate–quartz hydrothermalites with pyrite, arsenopyrite, and gold dissemination) and propylitization (chlorite, sericite, and pyrite). The veins are of essentially quartz, quartz–carbonate, and, seldom, carbonate composition. Quartz is a predominant vein mineral (90 vol.%). Calcite, chlorite, sericite, albite, kaolinite, K–Na-feldspar, and adularia are minor. The amount of calcite–quartz material in the ores seldom exceeds 5–10 wt.%. The ore minerals are arsenopyrite (prevailing), pyrite, and native gold; sphalerite and galena are subordinate; and chalcopyrite, ilmenite, rutile, scheelite, and apatite are scarce. The total amount of ore minerals is no more than 0.5–1.0 wt.% (Goncharov et al., 2002).

The ore-bearing rocks of the Pavlik deposit are characterized by normal alkalinity (NAI = 0.35) with a predominance of potassium (AI = 0.66) (Table 1).

Analysis of the sulfur isotope composition of arsenopyrite and pyrite from the ores of the two deposits showed close $\delta^{34}S$ values: –3.4 to –3.8‰ (Natalka) and –2.8 to –3.5‰ (Pavlik), which suggests a crustal source of sulfur.

The ore-bearing rocks of the deposits have high contents of chalcophile elements Au, Ag, As, W, and Sb and near-clarke contents of Pb, Cu, Zn, Ni, and Co relative to their average contents in the upper continental crust (Taylor and McLennan, 1985) and in the unaltered Permian rocks of the Tikhonya Brook (Table 2). Note that the rocks of the Pavlik deposit are orders of magnitude richer in Bi than those of the Natalka deposit. A similar specific feature was established for the Rodionovskoe gold deposit (Volkov et al., 2016).

Geochemical associations in the Natalka and Pavlik ores were identified by calculation of element correlations at a 99% confidence level (Smagunova and Karpukova, 2012). The geochemical associations typical of the Natalka deposit are as follows: (1) strong correlation between Au and ore-indicative elements Pb–Bi–W, (2) Co–Zn–Cu, (3) Ni–Sn–Ag (and a weaker correlation with Mo), (4) As–Sb, and (5) Se–Te. The geochemical associations specific to the Pavlik deposit are: (1) Ag–Au, (2) Co–Zn–Ni–Pb–Mo–Sn, and (3) W–Sb–Se (and a weaker correlation with Cu).

REE patterns of the unaltered late Permian rocks. Table 2 presents the determined contents of REE in the unaltered sedimentary and volcanosedimentary rocks of the Tikhonya Brook and in the hydrothermally metamorphosed rocks of the Natalka and Pavlik gold deposits.

*The Tikhonya Brook section***.** To determine the composition of sedimentary rocks and the redox conditions of their formation, we used the following efficient techniques: (1) comparison of the composition of clay shales and mudstones with the composition of the PAAS, NASC, ES, or RPSC geochemical standards; (2) analysis of the behavior of the Eu/Eu* and Ce/Ce* anomalies; and (3) analysis of the ratio of trace elements typical of acid or basic rocks in the clay shales and mudstones (Th/La, Nb/La, U/Th, and Co/Ni). The Eu/Eu* and Ce/Ce* anomalies are used to estimate the redox parameters of a solution, because these elements are present in two valence states (Bau, 1991).

The maximum total REE contents are found in the P_3om siltstones (173.25 ppm), and the minimum ones, in the P_3at diamictites (63.67 ppm). The LREE/HREE ratios in the P_3at rocks vary from 4.9 to 9.3, averaging 7.57 ($(La/Yb)_N$ = 6.76–9.00). The highest REE fractionation is observed in the deposits of the Omchak Formation, where LREE/HREE varies from 5.2 to 11.16, averaging 8.60 ($(La/Yb)_N$ = 8.27–16.83).

The P_3om deposits are enriched in LREE and show a well-pronounced negative Eu anomaly (Eu/Eu* = 0.60), which is close to the average Eu/Eu* value in the PAAS (0.66). The P_3at rocks show a LREE fractionation and a weak negative Eu anomaly (Eu/Eu* = 0.79). Cerium anomaly (Ce/Ce*) is not pronounced in the unaltered rocks. The analyzed samples from the Tikhonya Brook are slightly depleted in LREE relative to the PAAS (Nance and Taylor, 1976) (Table 3).

The unaltered rocks of the Tikhonya Brook are characterized by Eu/Eu* < 1, which indicates a predominance of Eu^{3+} and, accordingly, the relatively oxidizing conditions of sedimentation.

Monazite (kularite), Nd-monazite, and xenotime are REE-concentrating minerals. In the P_3om rocks, REE phosphates are represented by oval and rounded monazite grains with a shagreen surface, 47–93 μm in size; the monazite

Table 3. Average REE contents in the sedimentary and volcanosedimentary rocks of the Tikhonya Brook and in the ores of the Natalka and Pavlik gold deposits, ppm

Element	PAAS	Atkan Formation			Omchak Formation				Natalka deposit					Pavlik deposit				
		Average	Silty mudstone	Diamictite	Average	Mudstone	Siltstone	Sandstone	Average	Group				Average	Group			
										I	II	III	IV		I	II	III	IV
	20*	8	2	6	16	4	9	3	24	6	7	9	2	22	12	7	2	1
La	38.0	11.65	18.38	10.30	30.37	20.52	34.06	32.44	11.36	19.90	13.05	6.27	2.73	28.05	31.71	30.01	10.75	5.03
Ce	80.0	27.07	40.52	24.38	64.05	44.86	71.03	68.72	24.60	42.81	28.69	13.43	5.89	58.19	66.08	61.67	22.62	10.32
Pr	8.9	3.52	5.07	3.21	7.90	5.71	8.76	8.24	3.05	5.07	3.74	1.67	0.73	6.68	7.54	7.15	2.61	1.22
Nd	32.0	15.24	20.87	14.11	31.04	23.86	33.80	32.34	12.94	21.08	16.28	7.10	3.09	24.84	27.86	26.79	10.05	4.60
Sm	5.6	3.33	4.33	3.13	6.15	5.23	6.46	6.43	2.78	4.35	3.67	1.51	0.63	4.42	4.88	4.85	1.99	0.82
Eu	1.1	0.81	0.96	0.78	1.16	1.16	1.17	1.14	0.70	1.06	0.96	0.39	0.14	0.90	0.98	1.00	0.50	0.19
Gd	4.7	3.01	3.92	2.83	5.90	5.09	6.25	5.93	2.46	3.48	3.50	1.39	0.57	4.27	4.69	4.65	2.08	0.86
Tb	0.8	0.38	0.46	0.36	0.78	0.70	0.83	0.73	0.28	0.46	0.37	0.15	0.06	0.46	0.50	0.50	0.22	0.08
Dy	4.4	1.81	2.01	1.77	4.01	3.70	4.30	3.57	1.34	2.26	1.67	0.70	0.26	2.07	2.28	2.24	1.04	0.37
Ho	1.0	0.35	0.38	0.34	0.80	0.72	0.87	0.69	0.23	0.40	0.29	0.12	0.04	0.39	0.43	0.42	0.19	0.07
Er	2.9	1.09	1.25	1.05	2.36	2.04	2.60	2.08	0.73	1.30	0.86	0.38	0.13	1.20	1.36	1.25	0.59	0.24
Tm	0.4	0.17	0.20	0.16	0.34	0.29	0.38	0.31	0.10	0.18	0.12	0.05	0.02	0.17	0.19	0.18	0.08	0.04
Yb	2.8	1.12	1.38	1.07	2.10	1.67	2.34	1.94	0.75	1.38	0.86	0.39	0.14	1.19	1.37	1.19	0.55	0.26
Lu	0.4	0.20	0.24	0.19	0.34	0.26	0.39	0.33	0.12	0.22	0.14	0.06	0.02	0.19	0.22	0.19	0.09	0.04
Σ REE	183.0	69.72	99.97	63.67	157.32	115.78	173.25	164.88	61.44	103.95	74.20	33.61	14.46	133.01	150.07	142.08	53.38	24.13
$(La/Yb)_N$	9.15	7.13	9.00	6.76	13.66	8.27	16.83	11.33	10.71	9.74	10.00	11.00	13.21	15.53	15.58	16.43	13.16	13.30
$(Gd/Yb)_N$	1.34	2.29	2.30	2.29	3.18	2.47	3.73	2.48	2.87	2.07	3.34	2.98	3.34	2.90	2.77	3.07	3.04	2.72
LREE/ HREE	9.68	7.57	9.29	7.23	8.60	7.35	8.79	9.71	9.40	9.83	8.65	9.43	10.55	12.33	12.63	12.55	10.21	11.50
Eu/Eu*	0.66	0.79	0.71	0.80	0.60	0.70	0.57	0.57	0.82	0.86	0.83	0.82	0.72	0.64	0.63	0.63	0.75	0.69
Ce/Ce*	1.07	1.08	1.07	1.08	1.05	1.05	1.05	1.05	1.04	1.05	1.04	1.03	1.04	1.06	1.07	1.04	1.06	1.04

Note. $Eu/Eu^* = Eu_N \times (Sm_N \times Gd_N)^{1/2}$ (Taylor and McLennan, 1985), $Ce/Ce^* = Ce_N/((2La_N + Sm_N)/3)$ (Evensen et al., 1978), where *N* marks chondrite-normalized values. The analyses were carried out by ICP MS at the Institute of Tectonics and Geophysics, Khabarovsk.

contains Ce and La oxides. The deposits of the Atkan and Omchak formations contain lumpy-angular Nd-monazite grains 28–70 μm in size, sometimes with a ThO_2 impurity, and xenotime grains with Dy_2O_3, Er_2O_3, and Gd_2O_3 impurities (Mikhalitsyna and Sotskaya, 2016).

To assess the redox conditions in the late Permian sedimentary basin, we used the U/Th_{av} and Co/Ni_{av} indices (Jones and Manning, 1994; Kun et al., 2014).

In an oxidizing medium, U/Th ≤ 0.75; in an anoxic medium, U/Th = 0.75–1.25; and in a reducing medium, U/Th > 1.25. The Co/Ni < 1 value indicates a low temperature of mineralization, and Co/Ni > 1.5 points to a relatively high temperature of mineralization with the participation of a magmatic fluid (Jones and Manning, 1994; Kun et al., 2014).

The U/Th_{av} value is 0.27 and 0.20 in the unaltered rocks of P_3at and P_3om, respectively, which is close to the upper-crust value (0.25 in the PAAS) and indicates the oxidizing conditions of sedimentation. The Co/Ni ratios vary from 1.11 in the fine-grained rocks to 2.11 in the diamictites of P_3at and from 1.17 in the sandstones to 1.50 in the mudstones of P_3om. The high Co/Ni values in the diamictites of the Atkan Formation suggest the contribution of a magmatic source to their formation.

REE patterns of the ores of the Natalka and Pavlik gold deposits. The REE patterns are chondrite-normalized (Fig. 2). To estimate the behavior of REE during the ore-forming process, we normalized the REE contents of hydrothermally altered rocks to the background REE contents of the primary rocks (Tikhonya Brook) (Fig. 2).

The analyzed ore-bearing rocks of the deposits are of the same structural and chemical types and are tentatively divided into four groups: Group I (weakly altered rocks) comprises carbonaceous clay shales and siltstones with rare sulfide dissemination (<1%), tuffaceous-material impurity (≤5%), and single quartz and carbonate breakthroughs; group II (beresites) is siltstones with sulfide dissemination (~3%) and quartz and carbonate veinlets; group III is silicified and brecciated rocks; and group IV is veined quartz.

The maximum total REE contents are found in the weakly altered rocks (group I) of the Natalka and Pavlik gold deposits (103.95 and 150.07 ppm, respectively), and the minimum ones, in the vein quartz (group IV) (14.46 and 24.13 ppm, respectively). The average total REE content in the deposit ores is lower than that in the host rocks (Table 3).

All hydrothermally altered rocks are enriched in LREE. The highest LREE/HREE values are determined in the ore-bearing rocks of the Pavlik deposit, 10.21–12.63 (the average is 12.33) ($(La/Yb)_N$ = 13.16–16.43). In the rocks of the Natalka deposit, the LREE/HREE value varies from 8.65 to 10.55, averaging 9.40 ($(La/Yb)_N$ = 9.74–13.21).

The average REE contents in the deposit ores are much lower than those in the PAAS (Taylor and McLennan, 1985); the ores of the Pavlik deposit show high LREE/HREE values (Table 3).

The Eu/Eu* value in the rocks of the Pavlik deposit varies from 0.41 to 0.90, averaging 0.64, which is close to the average values of the continental crust (PAAS, Eu/Eu* = 0.66) and P_3om deposits (Eu/Eu* = 0.60) (Tikhonya Brook). The Eu/Eu* value in the rocks of the Natalka deposit varies

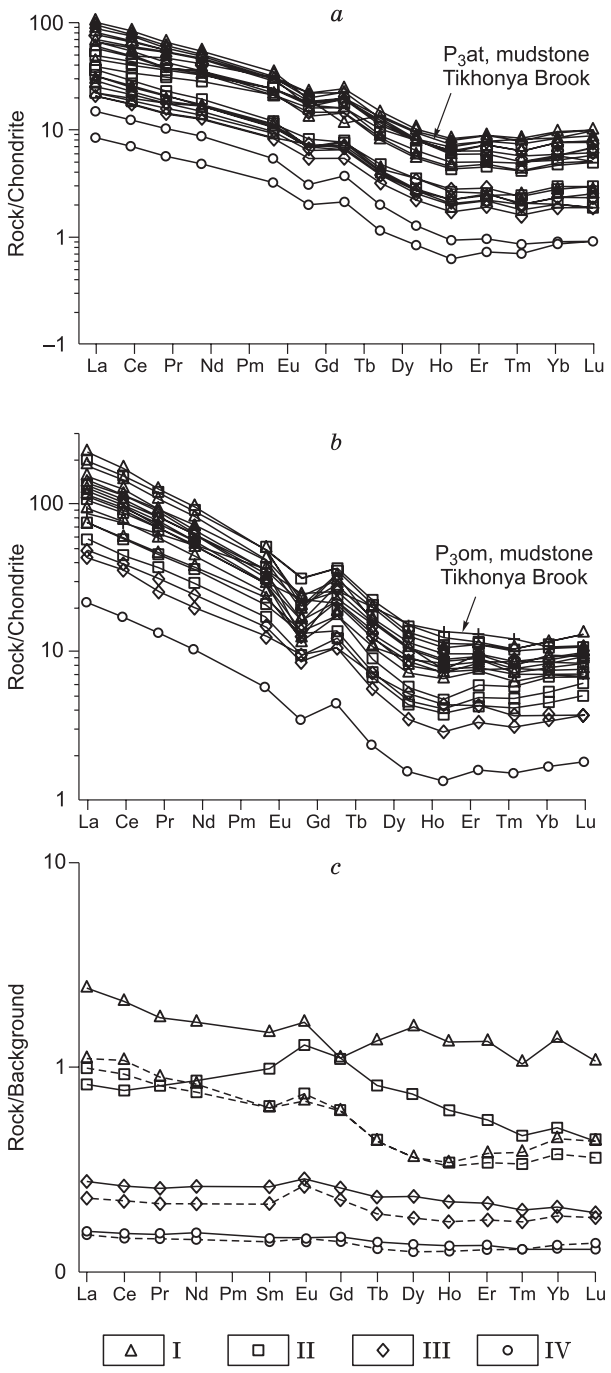

Fig. 2. Chondrite-normalized REE patterns of ore and unaltered rocks from the deposits: *a*, Natalka, *b*, Pavlik: I, weakly altered rocks, II, beresites (metasomatized rocks) with inclusions of cubic pyrite and quartz veinlets, III, silicified and brecciated rocks, IV, vein quartz; *c*, REE patterns normalized to the Tikhonya Brook rocks (Natalka deposit (solid line) and Pavlik deposit (dashed line)).

from 0.68 to 1.01, averaging 0.82, which is close to that of the P_3at deposits (Tikhonya Brook) and is higher than the average Eu/Eu* value of the PAAS.

The Ce/Ce* values of the studied samples are close to the background ones (Table 3), averaging 1.04 at the Natalka deposit and 1.06 at the Pavlik deposit. The Eu/Eu* values are mostly lower than unity, which indicates a predominance of Eu^{3+} and the contribution of a relatively oxidizing fluid to their formation. The Eu/Eu* increase to 1.01 in some samples indicates a slight reduction of the mineral-forming fluid (Anan'ev, 2012).

The ores of the Natalka and Pavlik deposits are characterized by U/Th < 0.75 (0.16–0.20) (Table 2), which indicates their formation under oxidizing conditions. The Co/Ni index in the Natalka ores is smaller than 1.5 (0.45–1.23); such values are typical of low and moderate ore formation temperatures. The Co/Ni index in the Pavlik ores is significantly lower, 0.11–0.59, thus indicating a low temperature of ore-bearing fluids. In general, the data obtained are in agreement with the results of previous studies (Savchuk et al., 2018).

As shown earlier (Oreskes and Einaudi, 1990; Kun et al., 2014), Cl-enriched hydrothermal fluids perfectly concentrate LREE but are poor in HREE, with their Nb/La and Th/La values being smaller than unity, whereas F-enriched hydrothermal fluids concentrate both LREE and HREE, and their Nb/La and Th/La values are usually greater than unity (Oreskes and Einaudi, 1990; Kun et al., 2014). The ores of both deposits are characterized by Nb/La and Th/La values smaller than unity (Table 2), which is typical of the hydrothermal NaCl–H_2O system enriched in Cl relative to F.

The REE patterns normalized to the primary rocks (Tikhonya Brook) show a redistribution of REE: The weakly altered rocks of the Natalka deposit are enriched in REE, and those of the Pavlik deposits, in LREE only. The beresites are characterized by the input of MREE (detected in the Natalka ores) and the removal of other REE. The silicified metasomatites, quartz breccias, and vein quartz from both deposits show almost identical REE patterns, which probably confirms the common nature of hydrothermal fluids (Fig. 2).

Thus, both gold deposits formed with a change in REE contents. All studied rocks demonstrate similar REE patterns: They are enriched in LREE and lack a Ce anomaly (0.95 < Ce/Ce* < 1), which indicates an insignificant role of oxidized meteoric waters in the formation of mineralization. The weak Eu anomaly (Eu/Eu* < 1) indicates a relatively oxidized fluid with a predominance of Eu^{3+} (Anan'ev, 2012). The Eu/Eu* increase in the P_3at volcanosedimentary rocks (0.82–0.86) suggests a magmatic source of REE.

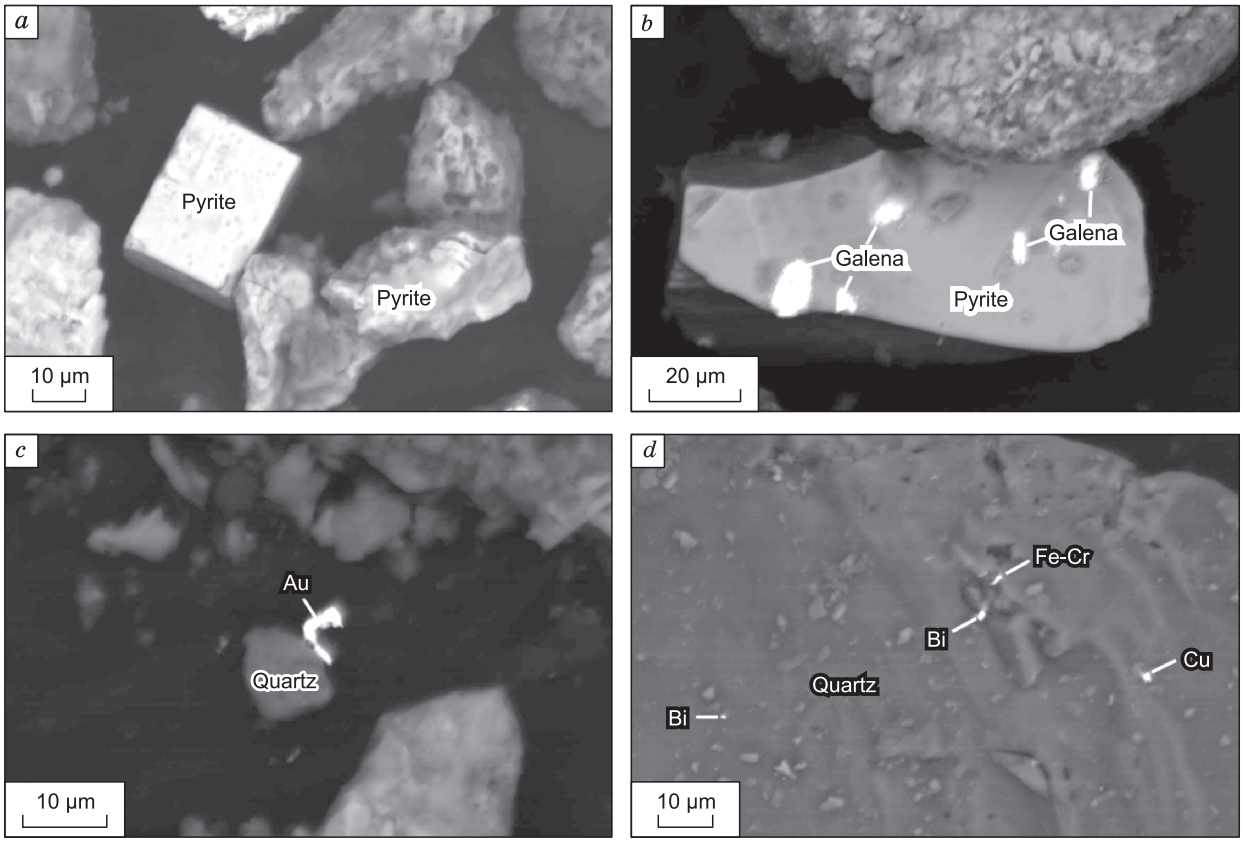

Fig. 3. Ore mineralization in the P_3at rocks of the Tikhonya Brook: *a*, Cubic crystal and irregular-shaped pyrite grain (sample 2-8); *b*, galena microinclusions in pyrite; *c*, native gold (sample 2-4); *d*, microinclusions of native bismuth and copper and Fe–Cr inclusion in quartz (sample 2-2).

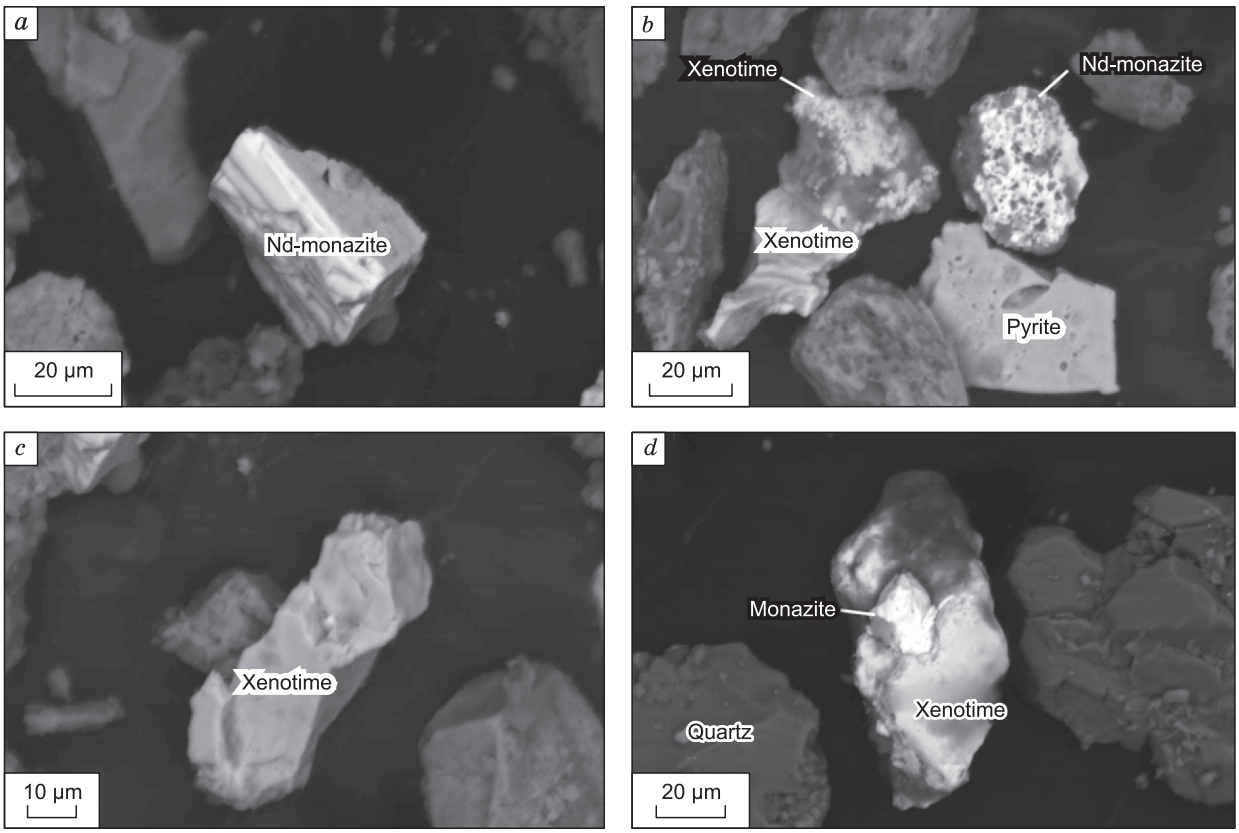

Fig. 4. REE-minerals in the P_3at rocks of the Tikhonya Brook: *a*, Prismatic Nd-monazite crystal; *b*, Nd-monazite and xenotime grains; *c*, intergrowths of bipyramidal xenotime crystals (*a*–*c*, sample 2-8); *d*, intergrowth of monazite and xenotime grains (sample 2-4).

Micromineralogy. *The Atkan Formation (Tikhonya Brook)*. A comprehensive study of the diamictites of the Atkan Formation revealed sulfides: pyrite, arsenopyrite, galena, and sphalerite. Pyrite is present as cubic crystals and irregular-shaped grains 20–52 μm in size (Fig. 3*a*). Sphalerite and galena are rare. Galena occurs as cubic crystals measuring up to 20 μm and their intergrowths and also as elongate microinclusions 4–12 μm in size in pyrite grains (Fig. 3*b*). There are also a single grain of native gold, 2–4 μm in size (Fig. 3*c*), and microinclusions of native bismuth, up to 2 μm in size. The silty mudstones contain marcasite, single inclusions of native bismuth (0.8–1.2 μm) and native copper (1.2 μm), and a Fe–Cr inclusion (2.6 μm) (Fig. 3*d*).

Nd-monazite and xenotime often occur in diamictites. Nd-monazite is present both as thick-tabular prismatic crystals 30–53 μm in size and their intergrowths (Fig. 4*a*) and as lumpy-angular grains. According to the EPMA data, the content of Nd_2O_3 in monazite varies from 7.79 to 31.73 wt.% (Table 4). Xenotime (20–70 μm) is present as lumpy grains with angular edges and also as short-columnar and bipyramidal crystals (Fig. 4*b*–*d*). It contains 7.07–10.54 wt.% Dy_2O_3, 4.35–4.93 wt.% Er_2O_3, and 3.73–7.46 wt.% Gd_2O_3 (Table 4). Sometimes, there is a ThO_2 impurity (3.46–7.21 wt.%) in monazite and xenotime. In addition to individual large grains, REE- minerals are present as microinclusions ~3 μm in size in the intergrowths of their grains with sericite, chlorite, and rutile. There are also intergrowths of monazite (23 μm) and xenotime (75 μm) grains (Fig. 4*d*).

The fine-grained rocks (silty mudstone) also contain REE phosphates (Nd-monazite and xenotime). The Nd-monazite has compact elongate and isometric lumpy-angular grains measuring 28–70 μm. The content of Nd_2O_3 varies from 11.51 to 21.12 wt.%. There is often a ThO_2 impurity (3–6 wt.%) (Table 4). The xenotime has tetragonal–bipyramidal grains 36–100 μm in size with impurities (wt.%) of Dy_2O_3 (7.37–7.89), Er_2O_3 (4.49–4.51), and Gd_2O_3 (3.83–4.08) (Table 4).

The Omchak Formation (Tikhonya Brook). The siltstones contain sulfides pyrrhotite (43–85 μm) and arsenopyrite (40 μm) (Fig. 5*a*, *b*), zircon grains (Fig. 5*a*), and single galena grains.

REE phosphates are represented by monazite (kularite) and Nd-monazite (Fig. 5*c*, *d*). The kularite (47–93 μm) has lumpy, oval, and rounded grains with a shagreen surface and contains only Ce and La oxides (Fig. 5*c*). The Nd-monazite has compact grains with 22.10–31.47 wt.% Nd_2O_3 (Fig. 5*d*; Table 4). In addition to REE phosphates, one siltstone sample contains Ce-allanite (Ce_2O_3 = 12–13 wt.%, La_2O_3 ≈ 7 wt.%) grains measuring 47–121 μm (Table 4).

Table 4. Composition of REE-minerals in the rocks of the Atkan and Omchak formations of the Tikhonya Brook, wt.%

No.	Ce_2O_3	La_2O_3	Nd_2O_3	ThO_2	Y_2O_3	Dy_2O_3	Er_2O_3	Gd_2O_3	P_2O_5	Total
Silty mudstone **(Atkan Formation, Tikhonya Brook, sample 2-2)**										
1	29.25	13.11	16.33	6.17	—	—	—	—	35.14	100.00
2	36.77	18.13	11.51	—	—	—	—	—	33.58	100.00
3	28.63	12.77	21.12	3.82	—	—	—	—	33.67	100.00
4	—	—	—	—	41.10	7.89	4.49	4.08	42.44	100.00
5	—	—	—	—	39.47	7.37	4.51	3.83	44.82	100.00
Diamictite **(Atkan Formation, Tikhonya Brook, sample 2-1)**										
6	34.24	22.44	7.79	—	—	—	—	—	35.53	100.00
7	34.85	20.22	9.74	—	—	—	—	—	35.19	100.00
8	35.62	11.73	17.39	—	—	—	—	—	35.26	100.00
9	28.68	8.02	26.29	—	—	—	—	—	37.02	100.00
10	35.78	18.91	9.76	3.46	—	—	—	—	32.09	100.00
11	29.88	14.07	14.80	7.21	—	—	—	—	34.04	100.00
12	32.75	17.25	12.70	4.22	—	—	—	—	33.08	100.00
13	—	—	—	—	38.54	7.71	4.52	4.49	44.73	100.00
14	—	—	—	—	42.69	7.07	4.63	6.99	38.61	100.00
Diamictite **(Atkan Formation, Tikhonya Brook, sample 2-4)**										
15	34.75	18.19	11.39	—	—	—	—	—	35.67	100.00
16	32.26	17.40	17.06	—	—	—	—	—	33.28	100.00
17	27.55	9.49	28.39	—	—	—	—	—	34.57	100.00
18	28.57	16.75	18.07	4.32	—	—	—	—	32.29	100.00
19	28.29	12.42	19.59	5.16	—	—	—	—	34.53	100.00
20	—	—	—	—	41.56	7.57	4.63	3.80	42.44	100.00
21	—	—	—	—	40.00	7.66	4.62	3.90	43.83	100.00
22	—	—	—	—	42.35	8.37	4.74	4.78	39.77	100.00
23	—	—	—	—	40.54	7.80	4.57	4.52	42.57	100.00
Diamictite **(Atkan Formation, Tikhonya Brook, sample 2-8)**										
24	33.10	18.83	16.50	—	—	—	—	—	31.57	100.0
25	31.33	14.85	18.71	—	—	—	—	—	35.11	100.0
26	25.53	8.93	31.73	—	—	—	—	—	33.81	100.0
27	—	—	—	—	48.34	8.54	4.93	3.73	34.46	100.0
28	—	—	—	—	49.47	8.90	4.35	5.50	31.78	100.0
29	—	—	—	—	45.36	10.54	4.71	7.46	31.93	100.0
Coarse-grained sandstone **(Omchak Formation, Tikhonya Brook, sample 2-37)**										
30	50.28	15.86	—	—	—	—	—	—	33.86	100.0
31	47.61	17.44	—	—	—	—	—	—	34.95	100.0
32	44.52	23.48	—	—	—	—	—	—	32.00	100.0
33	47.40	20.93	—	8.70	—	—	—	—	22.97	100.0
34	21.79	6.75	37.38	—	—	—	—	—	34.08	100.0
35	36.41	12.07	24.29	—	—	—	—	—	27.23	100.0
36	29.02	14.79	20.28	9.03	—	—	—	—	26.88	100.0
37	—	—	—	—	59.03	6.84	3.36	2.33	28.44	100.0
38	—	—	—	—	53.67	8.19	3.89	3.76	30.49	100.0
Siltstone **(Omchak Formation, Tikhonya Brook, sample 2-38)**										
39	45.77	12.77	—	—	—	—	—	—	41.46	100.0
40	47.33	19.03	—	—	—	—	—	—	33.64	100.0
41	43.79	23.33	—	—	—	—	—	—	32.88	100.0

(*continued on next page*)

Table 4 (*continued*)

No.	Ce_2O_3	La_2O_3	Nd_2O_3	ThO_2	Y_2O_3	Dy_2O_3	Er_2O_3	Gd_2O_3	P_2O_5	Total
42	42.92	30.69	—	—	—	—	—	—	26.39	100.0
43	32.59	8.93	31.47	—	—	—	—	—	27.01	100.0
44	30.26	14.31	22.10	6.64	—	—	—	—	26.69	100.0
Siltstone **(Omchak Formation, Tikhonya Brook, sample 2-17)**										
45	13.31	6.92	11.83	14.58	22.60	27.76	3.00	100.0		
46	12.28	6.90	11.56	12.76	24.86	28.64	3.00	100.0		

Note. Dash, not found.

The studied coarse-grained sandstones contain pyrrhotite (40–50 μm), zircon, and REE phosphates (monazite (kularite), Nd-monazite, and xenotime). The kularite, containing Ce and La oxides, has lumpy oval and rounded grains (47–93 μm) with a shagreen surface. The Nd-monazite (Nd_2O_3 = 20.28–37.38 wt.%) has compact lumpy grains (Table 4), seldom with a ThO_2 impurity (8.70–9.03 wt.%). The xenotime (46–90 μm) has thick-tabular and elongated prismatic grains with impurities (wt.%) of Dy_2O_3 (6.84–8.19), Er_2O_3 (3.36–3.89), and Gd_2O_3 (2.33–3.76) (Table 4).

Streaky–disseminated ores of the Natalka and Pavlik gold deposits. Sulfide minerals of streaky-disseminated ores form fine dissemination, or, more seldom, clusters (5–10 mm) in rocks. The main heavy-fraction minerals are arsenopyrite and pyrite. Arsenopyrite occurs as prismatic, flattened hexagonal, and rhombic crystals and their fragments. Pyrite forms clusters of euhedral cubic and pentagon–dodecahedral crystals, often with an As impurity (up to 6.0%).

In addition to pyrite and arsenopyrite, the ores contain galena, chalcopyrite, sphalerite, scheelite, and rutile; sometimes, monazite and xenotime are present. Galena forms fine dissemination (measuring few microns) in arsenopyrite, pyrite, and sphalerite as well as intergrowths with cobaltite and

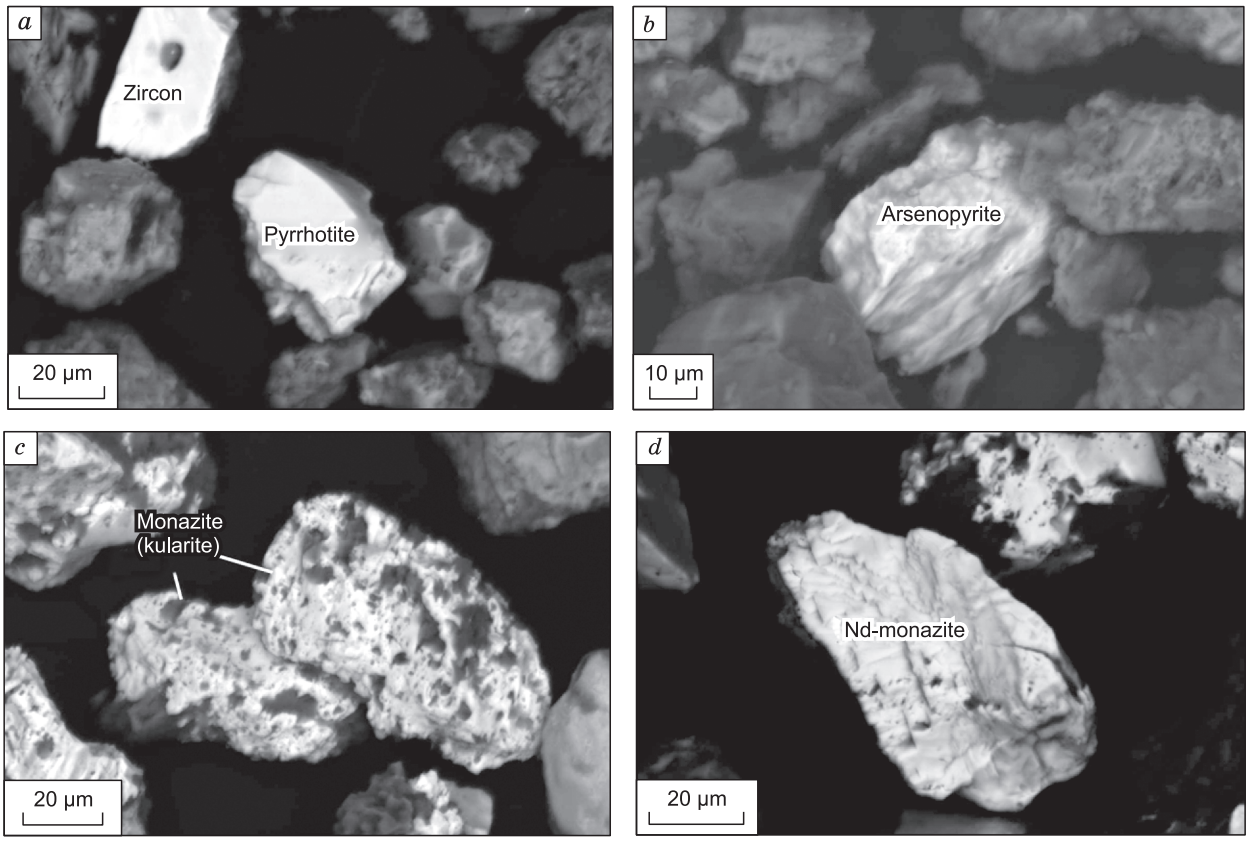

Fig. 5. Ore and REE mineralization in the P_3om deposits of the Tikhonya Brook: *a*, Elongate pyrrhotite grain; *b*, pseudopyramidal arsenopyrite grain (*a*, *b*, sample 2-17); *c*, monazite (kularite) grains; *d*, Nd-monazite grain (sample 2-38).

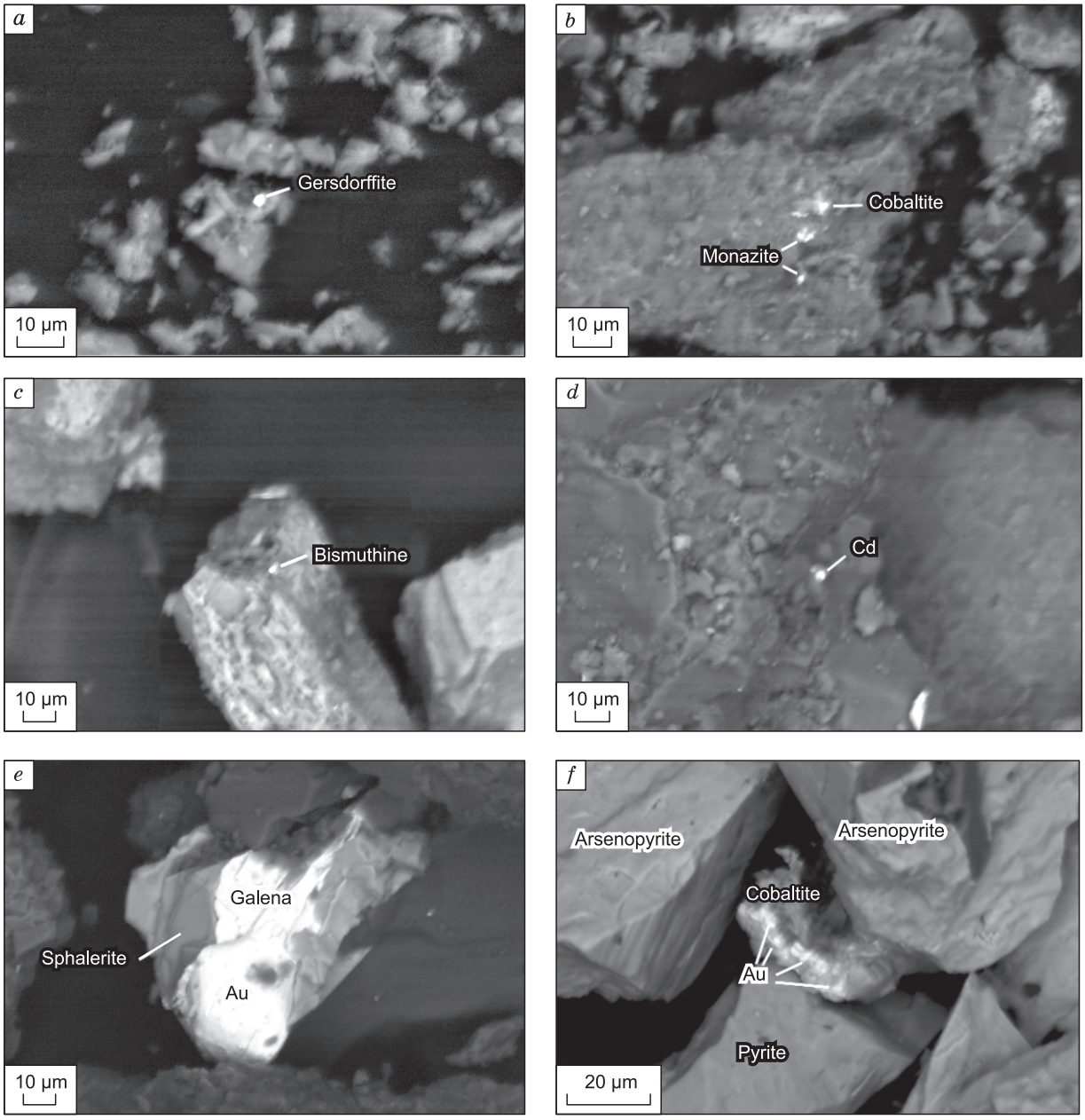

Fig. 6. Microinclusions in the Natalka ores: *a*, Gersdorffite; *b*, cobaltite; *c*, bismuthine; *d*, native cadmium in silicate matrix; *e,* intergrowth of gold, galena, and sphalerite; *f*, filmed gold in assemblage with colbaltite.

gold; sometimes, it is present as individual cubic crystals (up to 60 μm).

Native gold is the main commercially valuable component of the deposits. It is present in different forms, from microscopic rounded or, sometimes, irregular-shaped flakes and films to individual crystals and intergrowths. Gold microinclusions are found as fine (0.6–6 μm) dissemination in arsenopyrite and pyrite. Coarse grains of native gold (30–60 μm and larger) are irregular-shaped and lumpy. There are also rounded and angular gold grains, often branched; crystals with visible octahedral faces are rare. At the Natalka deposit, gold also occurs as intergrowths with galena, sphalerite (Fig. 6*e*), and scheelite and as fine dissemination in cobaltite (Fig. 6*f*).

The Natalka gold deposit. The deposit ores contain epitaxic intergrowths of galena and arsenopyrite, tabular and pseudo-octahedral scheelite crystals measuring 60–90 μm and their intergrowths (Sotskaya et al., 2012), and gersdorffite and cobaltite inclusions 2–3 μm in size, forming ingrowths in the rock matrix composed of sericite, albite, chlorite, ankerite, quartz, and ilmenite (Fig. 6*a*, *b*). The contents of Ni and Co in the gersdorffite are 27–30% and ~7%,

respectively; the cobaltite has a Ni impurity (~5–8%). In addition to fine inclusions of Ni and Co sulfoarsenides, there are single cubic and octahedral cobaltite crystals 20–35 μm in size, often intergrown with pyrite and arsenopyrite.

The cobaltite grains contain galena inclusions measuring 0.5 to 10–15 μm, and pyrite contains molybdenite flakes (7–14 μm) (Sotskaya et al., 2012). Most of the ore-bearing rocks (albite, sericite, and ankerite) have single inclusions of bismuthine (~1 μm) and native cadmium (2.6 μm) (Fig. 6*c*, *d*). Earlier, native cadmium was found as intergrowths with quartz of hydrothermal veins and veinlets and with chlorite and amphibole (containing 0.23–0.49% Cr) in the rocks of the South Verkhoyansk region. Probably, Cd formed at low temperature and pressure during the hydrothermal metasomatic alteration of terrigenous and carbonate rocks preceding the formation of streaky-disseminated mineralization (Lazebnik, 1984).

The REE mineralization of the Natalka deposit is represented by monazite and xenotime. Monazite microinclusions measuring 1–7 μm or, seldom, up to 10–15 μm are often present in arsenopyrite and pyrite grains and grain aggregates in the ore-bearing rocks (Fig. 6*b*) (Sotskaya et al., 2012). The monazite contains REE oxides, mainly Ce and La ones, and no impurities of other HREE, in contrast to the authigenic kularite found earlier in the Tikhonya Brook sediments (Nekrasova and Nekrasov, 1983; Tyukova et al., 2007). Xenotime present as single fine inclusions (2–4 μm) in the ore-bearing rocks has no REE impurities other than Y_2O_3 (Table 5).

The Pavlik gold deposit. The deposit ores contain Ni and Co minerals both as individual crystals and as intergrowths with sulfides. Cobaltite with Ni (3–4%) and Fe (6–9%) impurities occurs as inclusions (2–3 to 20 μm) in pyrite. Two ore samples contain inclusions (4–50 μm) of freibergite (with 6–28 wt.% Ag) intergrown with chalcopyrite, arsenopyrite, and pyrite (Fig. 7*a*).

Native gold occurs as isometric inclusions (0.6–6 μm) in arsenopyrite (Fig. 7*b*) and pyrite. The ores also contain sporadic intergrowths of Au–Ag selenide (fischesserite(?)) grains (0.6–2.5 μm) intergrown with arsenopyrite (Sotskaya et al., 2012).

The detected REE phosphates are monazite, Nd-monazite, and xenotime (Fig. 7*c*; Table 5). Their grains are of nearly the same shape and size as the REE phosphate grains from the Natalka gold deposit.

Rounded native-silver grains (1.1–5 μm) intergrown with arsenopyrite and, less often, arsenopyrite were found in the ores of both gold deposits. In addition, a single grain of Ag selenide (naumannite) was discovered at the Pavlik deposit, and silver telluride (hessite) grains measuring 2–59 μm were found at the Natalka deposit (Sotskaya et al., 2012).

Native gold and silver, Au and Ag selenides, and Ni and Co sulfoarsenides are present in assemblage with arsenopyrite and arsenous pyrite in the ores. Gold is often intergrown

Table 5. Composition of REE-minerals from the Natalka and Pavlik gold deposits, wt.%

No.	Ce_2O_3	La_2O_3	Nd_2O_3	Y_2O_3	P_2O_5	Total	Sample, deposit
Monazite							
1	43.22	25.31	—	—	31.47	100.00	N-11-2-33, Natalka
2	43.54	23.54	—	—	32.92	100.00	N-11-2-33, Natalka
3	46.18	22.56	—	—	31.26	100.00	1-2-33, Natalka
4	44.45	22.92	—	—	32.63	100.00	N-11-1-5, Natalka
5	47.02	21.10	—	—	31.88	100.00	N-11-1-5, Natalka
6	46.00	22.67	—	—	31.33	100.00	N-11-1-19, Natalka
7	46.20	22.77	—	—	31.03	100.00	N-11-1-19, Natalka
8	61.13	—	—	—	38.87	100.00	R-11-2-9, Pavlik
Nd-monazite							
9	17.73	—	41.31	—	40.96	100.00	R-11-2-9, Pavlik
10	25.62	—	35.45	—	38.93	100.00	R-11-2-9, Pavlik
11	34.57	—	26.38	—	39.05	100.00	R-11-2-9, Pavlik
12	27.74	—	36.98	—	35.28	100.00	R-11-2-9, Pavlik
13	29.59	—	33.87	—	36.54	100.00	R-11-2-9, Pavlik
Xenotime							
14	—	—	—	56.29	43.71	100.00	700072, Natalka
15	—	—	—	59.11	40.89	100.00	700072, Natalka
16	—	—	—	57.13	42.87	100.00	700003, Natalka
17	—	—	—	68.05	31.95	100.00	N-11-1-19, Natalka
18	—	—	—	69.62	30.38	100.00	R-11-2-9, Pavlik

Note. Dash, not found.

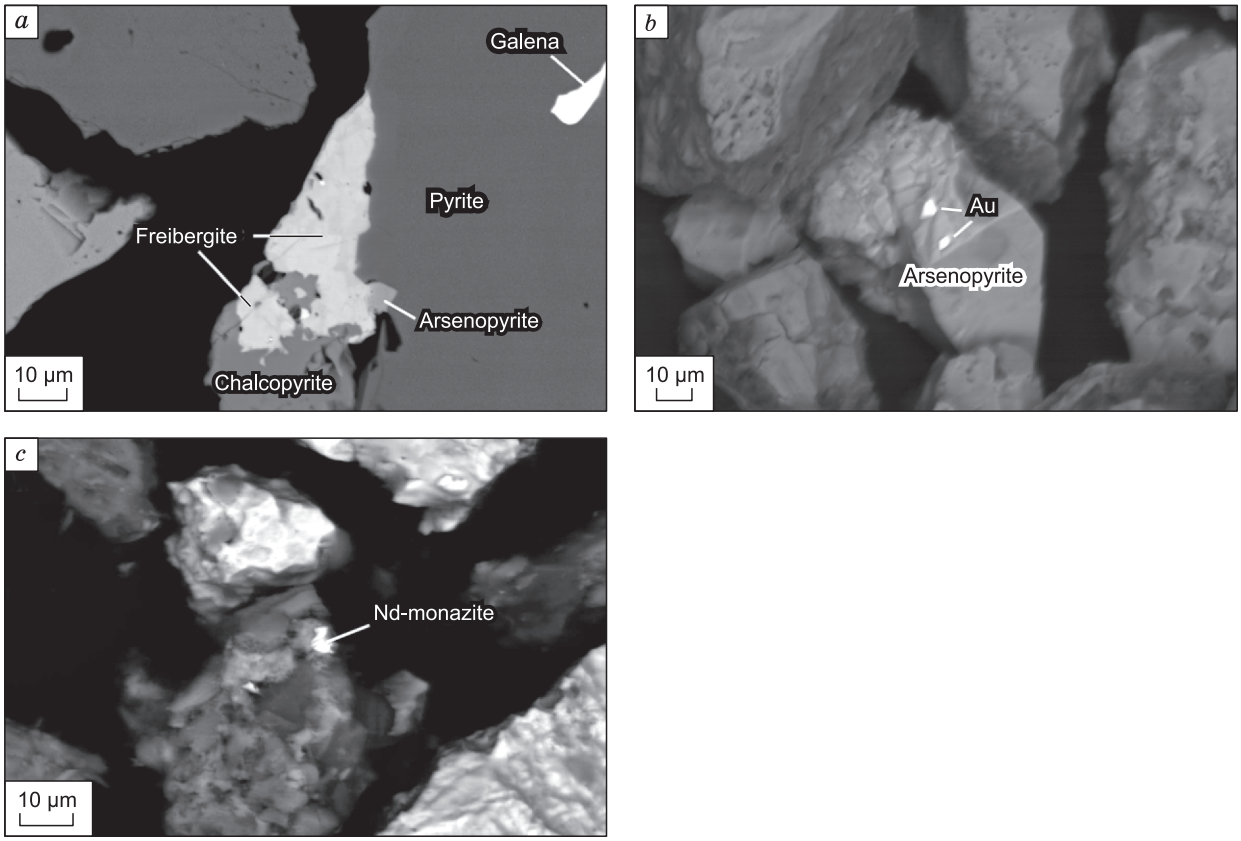

Fig. 7. Microinclusions in the Pavlik ores: *a*, Freibergite; *b*, gold intergrown with arsenopyrite; *c*, Nd-monazite.

with galena, scheelite, and cobaltite. In addition to coarse grains, native gold is widespread as microscopic drops, films, and veinlets.

DISCUSSION

The Permian rocks over the area under study underwent postdiagenetic and regional metamorphic transformations (the initial stage of the greenschist facies metamorphism). This led to a change in the mineralogical composition and structure of the late Permian rocks, namely, exfoliation, the appearance of dissolution structures in granular rocks under pressure, and the formation of carbonate, sericite, and disseminated sulfides. A large number of effusive fragments not resistant to dissolution under pressure led to the formation of conformal structures and the regeneration of fragments. The rocks show different degrees of exfoliation (the coarse-clastic rocks are weakly foliated, and the clayey ones are cleavaged). Dispersed pyritization is observed in all studied rocks.

The above data on petrochemical indices show minor variations in their values in the unaltered and ore-bearing rocks of the deposits. The most contrasting difference is observed for the hydrolysate index values: The unaltered rocks are siallites (clayey rocks), and the host rocks of the Natalka and Pavlik gold deposits are clay silicites (siliceous-clay shales). The studied rocks have normal titanium contents, which is typical of clayey rocks. The maximum alkali contents are observed in the rocks of the Atkan Formation (Tikhonya Brook) and Natalka gold deposit, which is due to the inflow of volcanic material into the sedimentation basin.

The Permian rocks of the Omchak Formation (P_3om) contain Ca–Mn carbonate minerals, which might have formed from biogenic carbonate. Many trace elements (Co, Cr, Pb, Zn, Mo, Ag, Sn, Fe, Cu, and Ti) accumulate in terrigenous deposits containing concentrating components, such as clay minerals, organic matter, iron and manganese hydroxides, and finely dispersed iron sulfides (McMurtry et al., 1991; Astakhov et al., 1995).

The ICP MS data show that the late Permian rocks of the Tikhonya Brook are enriched in Au, Ag, PGE, Co, Zn, Bi, and Pb and the ores of the Natalka and Pavlik gold deposits are enriched in As, Sb, W, Pb, Au, Ag, Pd, Ir, Bi, Cu, and Zn relative to the upper crust (Taylor and McLennan, 1988). The Bi enrichment of the Pavlik ores suggests the presence of a magmatogene fluid.

The Co/Ni ratio in the Pavlik ores is much smaller than unity, which is typical of a low mineralization temperature. The Natalka ores are characterized by Co/Ni = 0.45–1.23 corresponding to the low–moderate temperatures of the fluid ore formation.

The formation of gold deposits proceeds with a change in REE contents. The Natalka and Pavlik gold deposits show similar REE patterns. The rocks are enriched in LREE; $(La/Yb)_N$ increases from primary to hydrothermally and metasomatically transformed rocks. No Ce anomaly is observed, which indicates a minor contribution of oxidized meteoric waters to the ore formation.

The high Eu* anomaly in the P_3at volcanosedimentary rocks (0.82–0.86), the morphology of REE-mineral grains, the presence of Nd impurity in them, and the high Co/Ni ratios (>1.5, up to 2.11) confirm the presence of a magmatic fluid.

We have established that the gold deposits formed under different redox conditions (U/Th ≤ 0.75, Nb/La < 1, and Th/La < 1), mainly with the participation of a relatively oxidized fluid enriched in LREE of the hydrothermal system NaCl–H_2O, with domination of Cl over F.

Microminerals of ore-forming and associated elements are typical of ores of black-shale strata; some of them might be products of redeposition from the ore-bearing strata. The crucial role of the protoliths in the formation of mineralization is evidenced by the isotopic composition of sulfide sulfur suggesting its crustal nature and by the composition of the organic matter of rocks and ores indicating its sedimentary nature.

The Au and Ag contents in the Natalka and Pavlik ores are significantly higher than those in the late Permian rocks of the Tikhonya Brook. The abnormal As and W contents in the ores are due to the presence of arsenopyrite and scheelite.

At the Pavlik deposit, naumannite and fishesserite (Au and Ag selenides) were found at the faces of arsenopyrite crystals (Sotskaya and Goryachev, 2012). According to thermobarometric studies (Goncharov et al., 2002; Goryachev et al., 2008), the ores of the Natalka and Pavlik deposits formed at 220–350 ºC, which ensured the formation of mainly Ag and Au selenides because of the stronger affinity of Ag for Se rather than S at such *P–T* parameters of the fluid (Nekrasov, 1991). The scarcity of selenides is due to the low Se contents in the ore-bearing carbonaceous strata and, accordingly, in the fluid system of the gold deposits.

Electron microscope study of the unaltered rocks of the Tikhonya Brook showed that the P_3om deposits are poor in ore and REE mineralization (pyrrhotite, arsenopyrite, monazite, Nd-monazite, Ce-allanite, and xenotime). The P_3at rocks have a more diverse mineral composition: pyrite, arsenopyrite, galena, sphalerite, marcasite, native bismuth, copper, and gold, Fe–Cr inclusions, monazite, Nd-monazite, and xenotime, which mark their volcanosedimentary nature.

The REE phosphate with oval grains is usually called kularite. The authigenic monazite (kularite) examined earlier in the Permo–Triassic strata of the Kular Ridge (Nekrasova and Nekrasov, 1983) and at the Natalka gold deposit (Tyukova et al., 2007) have ellipsoidal or, more seldom, lumpy grains with a shagreen surface, 0.1–1.5 mm in size. The kularite described by Nekrasova and Nekrasov (1983) contains not only Ce and La but also Th (≤1.40 wt.%) and Eu (up to 2.19 wt.%), as well as Sm, Pr, Nd, Gd, Tb, and Dy. The kularite of the Natalka gold deposit contains Nd_2O_3, Pr_2O_3, Y_2O_3, and ThO_2 (Tyukova et al., 2007).

Monazite from the P_3om sediments of the Tikhonya Brook, having oval and rounded grains with a shagreen surface and containing Ce and La oxides, can be referred to as sedimentary kularite. There are also compact lumpy-angular grains of Nd-monazite and igneous xenotime in the P_3at and P_3om sediments.

In the streaky-disseminated ores of the Natalka and Pavlik gold deposits, REE phosphates (monazite and xenotime) are present as microinclusions in arsenopyrite, pyrite, and aggregates of metasomatites.

In addition to the morphologic difference, the above minerals have different chemical compositions: The monazite from streaky-disseminated ores contains only Ce and La oxides and no ThO_2 impurity, and the xenotime lacks Dy_2O_3, Er_2O_3, and Gd_2O_3. Since REE are most mobile during hydrothermal and metasomatic processes (Kolonin et al., 2001), they might dissolve and be redeposited from the host rocks in the ores. The intimate assemblage of the ore monazite with the minerals of metasomatized rocks and with sulfide minerals (pyrite and arsenopyrite) as well as its morphology and above-mentioned difference from xenotime in the set of impurities suggest its hydrothermal genesis. The intergrowths of monazite and xenotime with pyrite and arsenopyrite at the studied deposits suggest that REE migrated with hydrothermal fluids containing reduced sulfide sulfur (Giere, 1993). A minor part of REE migrated in the form of phosphate complexes, as evidenced by the high contents of P_2O_5 (Tikhonya Brook).

The REE and gold types of mineralization in other similar deposits are also of hydrothermal nature. Monazite in assemblage with pyrite, rutile, and apatite was found in the metasomatites of the Muruntau gold deposit, where a relationship between REE and gold minerals during the hydrothermal ore formation was established (Dunin-Barkovskaya, 2007). Microinclusions of native gold (about 2 μm in size) were found in Ce-allanite from the Chudnoe gold deposit (Sotskaya et al., 2014), which also indicates a relationship between REE and precious-metal minerals in the course of hydrothermal metasomatic processes. The same is evidenced by the revealed finest (4–5 μm) isometric inclusions of REE minerals (tissonite, Ce, La, and Nd oxides, and monazite) in the matrix of metasomatites from the Chertovo Koryto gold deposit, composed of fluorapatite (up to 7.5% F), ankerite, calcite, sericite, and albite (Tarasova et al., 2016).

The ores of the studied gold deposits often contain cobaltite and gersdorffite and, more seldom, bismuthine. Part of the Ni–Co-minerals was, most likely, inherited from the host rocks, and the other part formed during the rock formation.

CONCLUSIONS

Thus, the host late Permian carbonaceous strata participated in the formation of the Natalka and Pavlik gold deposits. This is evidenced by the redistribution of precious and

associated elements from the host and underlying rocks as a result of hydrothermal metasomatic processes and their concentration as new phases in ores.

The Permian rocks are characterized by supraclarke and near-clarke contents of Au, Ag, Co, Cu, Zn, Mo, Pb, Bi, and PGE relative to the upper crust.

The obtained data on the accessory minerals of the late Permian carbonaceous rocks showed that some of the ore elements form their own minerals. The ore minerals (pyrite, arsenopyrite, galena, sphalerite, and native bismuth, copper, and gold) revealed in the unaltered rocks with near-clarke contents of ore-forming elements suggest the presence of dispersed arsenic and bismuth minerals.

The local enrichment of the Permian Tikhonya Brook section (Mikhalitsyna, 2011; Goryachev et al., 2012) in trace elements Ni, Cr, and Co is confirmed by the presence of accessory minerals (native bismuth and copper, Fe–Cr intermetallic compounds) in the late Permian unaltered rocks and thus indicates their leading role in the ore formation of the Ayan–Yuryakh anticlinorium. Although Pt and Pd minerals were not found in the Natalka ores, the bead of these ores contains 1% Pt (Voroshin et al., 1995).

The analysis of the trace-element distribution in the deposit ores has shown their enrichment in chalcophile elements Au, Ag, As, W, and Sb relative to the average composition of the upper crust and the host Permian rocks. The high W and Bi contents in the ores suggest the involvement of a magmatic fluid in their formation.

The revealed microminerals of ore-forming and associated elements (Ni, Co, Sb, Mo, Cr, and Se) are typical of ores localized in black-shale strata. The fact that there are no abnormal contents of these elements indicates that they were redeposited from the ore-bearing strata but not supplied with ore-forming fluids. This is also evidenced from the isotopic composition of sulfide sulfur and the characteristics of carbonaceous ore material. As shown earlier, the host rocks are the main source of sulfur, whereas the deep-seated sources play a minor role (Goncharov et al., 2002; Tyukova and Voroshin, 2003; Goryachev et al., 2013).

The ore formation is accompanied by the destruction of rock-forming minerals and the removal of iron, which reacts with S, As, and Au supplied by solutions to form gold-bearing pyrite and arsenopyrite (Zakharevich et al., 1987). The rock metasomatism is accompanied by the removal of Au, which leads to an increase in its concentration in the solution (Letnikov and Vilor, 1981). Obviously, gold was deposited from hydrothermal solutions on sulfides (reduction barrier); thus, gold microparticles formed. Microscopic gold intergrown with arsenopyrite and pyrite was deposited simultaneously with disseminated sulfides.

Rare-earth element mineralization in assemblage with gold-bearing sulfides and sulfoarsenides is also widespread in the ores. Probably, the ore formation was accompanied by the active leaching of REE from primary minerals (aluminosilicates) and their subsequent migration in hydrothermal fluids, followed by the deposition of newly formed phases as finest segregations. All studied rocks have similar REE patterns: They are enriched in LREE and show no Ce anomaly, which suggests the inheritance of REE from the late Permian unaltered rocks.

We have established that the gold deposits formed under different redox conditions, mainly with the participation of a relatively oxidized fluid enriched in LREE of the hydrothermal system NaCl–H_2O, with domination of Cl over F.

The studies have shown that the host carbonaceous sedimentary complexes, which served as additional sources of precious and associated metals, played a crucial role in the formation of the Natalka and Pavlik gold deposits. This is evidenced from the obtained geochemical and microminer-alogical data on the redistribution of gold and associated elements during the formation of gold mineralization.

REFERENCES

Alpatov, V.V., Mikhalitsyna, T.I., 2000. Hydrothermal alteration of rocks at the Natalka gold deposit, in: Magmatism and Metamorphism in Northeastern Asia. Proceedings of the Fourth Regional Petrographic Workshop on Northeastern Russia [in Russian]. SVKNII DVO RAN, Magadan, pp. 281–284.

Anan'ev, Yu.S., 2012. Rare-earth elements in metasomatites and ores of the West Kalba gold deposits. Izvestiya Tomskogo Universiteta 321 (1), 56–62.

Ague, J.J., 2001. Transport of rare earth elements by fluids during Barrovian-style metamorphism. XI Goldschmidt Conference Abstracts, p. 3641.

Astakhov, A.S., Beloglazov, A.I., Mozherovskiy, A.V., 1995. Mineral-geochemical association in bottom sediments of the East China Sea. Terr. Atmos. Ocean. Sci. 6 (1), 91–102.

Astakhov, A.S., Goryachev, N.A., Mikhalitsyna, T.I., 2010. Conditions of the formation of gold-enriched horizons of ore-hosting black shale sequences (illustrated by Permian and recent marine sediments of Northeastern Asia). Dokl. Earth Sci. 430 (1), 9–14.

Balashov, Yu.A., 1976. Geochemistry of Rare-Earth Elements [in Russian]. Nauka, Moscow.

Barnett, E.S., Hutchinson, R.W., Adamcik, A., Barnett, R., 1982. Geology of the Agnico-Eagle gold deposit, Quebec, in: Hutchinson, R.W., Spence, C.D., Franklin, J.M. (Eds.), Precambrian Sulphide Deposits. Geol. Assoc. Can., Spec. Paper 25, pp. 403–426.

Bau, M., 1991. Rare earth element mobility during hydrothermal and metamorphic fluid–rock interaction and the significance of the oxidation state of europium. Chem. Geol. 93 (3–4), 219–230.

Biakov, A.S., Vedernikov, I.L., 1990. Stratigraphy of the Permian Deposits in the Northeastern Framing of the Okhotsk Massif and in the Central and Southeastern Parts of the Ayan–Yuryakh Anticlinorium. Preprint [in Russian]. SVKNII DVNTs AN SSSR, SVPGO, Magadan.

Biakov, A.S., Vedernikov, I.L., Akinin, V.V., 2010. Permian diamictites in Northeast Asia and their possible origins. Bulletin of the North-East Scientific Center of FEB RAS, No. 1, 14–24.

Bingen, B., Demaiffe, D., Hertogen, J., 1996. Redistribution of rare earth elements, thorium, and uranium over accessory minerals in the course of amphibolite to granulite facies metamorphism: The role of apatite and monazite in orthogneisses from southwestern Norway. Geochim. Cosmochim. Acta 60, 1341–1354.

Boyle, R.W., 1979. The geochemistry of gold and its deposits, in: Geological Survey of Canada, Bull. 280, pp. 412–423.

Buryak, V.A., 1982. Metamorphism and Ore Formation [in Russian]. Nedra, Moscow.

Buryak, V.A., Bakulin, Yu.I., 1998. Metallogeny of Gold [in Russian]. Dal'nauka, Vladivostok.

Buryak, V.A., Mikhailov, B.K., Parada, S.G., 1988. Metamorphism and Mineralization of Carbonaceous Strata in the Amur Area [in Russian]. DVNTs AN SSSR, Vladivostok.

Buryak, V.A., Mikhailov, B.K., Tsymbalyuk, N.V., 2002. Genesis, regularities of localization, and gold and platinum potential of black-shale strata. Rudy i Metally, No. 6, 25–36.

Button, A., 1976. Transvaal and Hamersley basins – Review of basin development and mineral deposits. Miner. Sci. Eng. 8 (4), 262–293.

Chanyshev, I.S., Stepanov, V.A., 1987. Distribution of gold and carbon in the Central Kolyma terrigenous strata and localization of gold mineralization. Litologiya i Poleznye Iskopaemye, No. 3, 112–118.

Davydov, V.I., Biakov, A.S., Isbell, J.L., Crowley, J.L., Schmitz, M.D., Vedernikov, I.L., 2016. Middle Permian U–Pb zircon ages of the glacial deposits of the Atkan Formation, Ayan–Yuryakh anticlinorium, Magadan province, NE Russia: Their significance for global climatic interpretations. Gondwana Res. 38, 74–85.

Dubinin, A.V., 2006. Geochemistry of Rare-Earth Elements in the Ocean [in Russian]. Nauka, Moscow.

Dunin-Barkovskaya, E.A., 2007. Paragenesis of REE-minerals and REE in the Kyzylkum gold deposits, in: The Role of Mineralogy in Understanding Ore Formation Processes. Proceedings of the Annual Session of the Moscow Department of the Russian Mineralogical Society Dedicated to the 110th Birthday of Academician A.G. Betekhtin (1897–2007) [in Russian]. IGEM RAN, Moscow, pp. 163–167.

Efremova, S.V., Stafeev, K.G., 1985. Petrochemical Methods of Rock Study [in Russian]. Nedra, Moscow.

Evensen, N.M., Hamilton, P.J., O'Nions, R.K., 1978. Rare earth abundances in chondritic meteorites. Geochim. Cosmochim. Acta 42, 1199–1212.

Gar'kovets, V.G., 1973. Identification of the Kyzylkum Type of Syngenetic–Epigenetic Deposits. Dokl. Akad. Nauk SSSR 208 (1), 306–310.

Giere, R., 1993. Transport and deposition of REE in H_2S-rich fluids: evidence from accessory mineral assemblages. Chem. Geol. 110, 251–268.

Gil'bert, A.E., Shatsky, V.S., Koz'menko, O.A., Orestova I.I., Sobolev N.V., 1988. Geochemistry of eclogites of some metamorphic complexes of the USSR. Dokl. Akad. Nauk SSSR 302 (1), 181–183.

Goncharov, V.I., Voroshin, S.V., Sidorov, V.A., 2002. The Natalka Gold Deposit [in Russian]. SVKNII DVO RAN, Magadan.

Goryachev, N.A., 2003. The Origin of the North Pacific Gold–Quartz Vein Belts [in Russian]. SVKNII DVO RAN, Magadan.

Goryachev, N.A., Vikent'eva, O.V., Bortnikov, N.S., Prokof'ev, V.Yu., Alpatov, V.V., Golub, V.V., 2008. The world-class Natalka gold deposit, Northeast Russia: REE patterns, fluid inclusions, stable oxygen isotopes, and formation conditions of ore. Geol. Ore Deposits 50 (5), 362–390.

Goryachev, N.A., Sotskaya, O.T., Mikhalitsyna, T.I., Goryacheva, E.M., Man'shin, A.P., 2012. Estimation of Au–Pt–Pd–Ni mineralization in the ores of the Natalka and Dogdekan deposits hosted by the black-shale strata of the Yana–Kolyma gold-bearing belt, in: Problems of Minerageny in Russia [in Russian]. GTs RAN, Moscow, pp. 325–336. http://nznews.wdcb.ru/ebooks/minerageny/

Goryachev, N.A., Kuznetsov, S.K., Sotskaya, O.T., Mayorova, T.P., Mikhalitsyna, T.I., 2013. Preconditions of the gold and platinoid association in ores from orogenic gold deposits. Bulletin of the North-East Scientific Center of FEB RAS, No. 4, 28–40.

Grauch, R.I., 1989. Rare earth elements in metamorphic rocks, in: Lipin, B.R., McKay, G.A. (Eds.), Geochemistry and Mineralogy of Rare Earth Elements. Rev. Mineral. 21, 147–167.

Hellman, P.L., Smith, R.E., Henderson, P., 1979. The mobility of the rare earth elements: Evidence and implications from selected terrains affected by burial metamorphism. Contrib. Mineral. Petrol. 71, 23–44.

Hutchinson, R.W., 1987. Metallogeny of Precambrian gold deposits; space and time relationships. Econ. Geol. 82 (8), 1993–2007.

Isbell, J.L., Biakov, A.S., Vedernikov, I.L., Gulbranson, E.L., Fedorchuk, N.D., 2016. Permian diamictites in northeastern Asia: Their significance concerning the bipolarity of the late Paleozoic ice age. Earth Sci. Rev. 154, 279–300.

Jones, B., Manning, D.A.C., 1994. Comparison of geochemical indices used for the interpretation of palaeoredox conditions in ancient mudstones. Chem. Geol. 111, 111–129.

Khanchuk, A.I. (Ed.), 2006. Geodynamics, Magmatism, and Metallogeny of Eastern Russia [in Russian]. Dal'nauka, Vladivostok, Book 1.

Kholodov, V.N., 1982. Novelty in learning of catagenesis. Elisional catagenesis. Litologiya i Poleznye Iskopaemye, No. 5, 15–32.

Kholodov, V.N., 2001. The role of a geochemical sedimentary process in the lithologic evolution, in: Problems of Lithology, Geochemistry, and Sedimentary Ore Genesis [in Russian]. MAIK "Nauka/Interperiodika", Moscow, pp. 54–92.

Kholodov, V.N., Shmariovich, E.M., 1992. Ore-generating processes of expelled and infiltration systems. Geologiya Rudnykh Mestorozhdenii, No. 1, 3–22.

Kokin, A.V., Sukhorukov, V.I., Shishigin, P.R., 1999. Regional Geochemistry (Southern Upper Yana Region) [in Russian]. RostIzdat, Rostov-on-Don.

Kolonin, G.R., Morgunov, K.G., Shironosova, G.P., 2001. A databank of stability constants of complex aqueous species of rare-earth elements in a wide range of temperatures and pressures. Geologiya i Geofizika (Russian Geology and Geophysics) 42 (6), 881–890 (829–839).

Konstantinov, M.M., 1993. Stratiform gold mineralization: achievements and problems of constructing models of ore-forming systems. Rudy i Metally, Nos. 1–2, 14–20.

Konstantinov, M.M., Kosovets, T.N., Orlova, G.Yu., Shchitova, V.I., Zhidkov, S.N., Slezko, V.A., 1988. Factors determining the localization of stratiform gold–quartz mineralization. Geologiya Rudnykh Mestorozhdenii, No. 5, 59–69.

Kun, L., Ruidong, Y., Wenyong, Ch., Rui, L., Ping, T., 2014. Trace element and REE geochemistry of the Zhewang gold deposit, southeastern Guizhou Province, China. Chin. J. Geochem. 33, 109–118.

Lazebnik, K.A. (Ed.), 1984. Rare Minerals in Yakutia [in Russian]. YaF SO AN SSSR, Yakutsk.

Letnikov, F.A., Vilor, N.V., 1981. Gold in a Hydrothermal Process [in Russian]. Nedra, Moscow.

Lottermoser, B.G., 1992. Rare earth elements and hydrothermal ore formation processes. Ore Geol. Rev. 7, 25–41.

McMurtry, G.M., DeCarlo, E.H., Kee Hyun Kim, 1991. Accumulation rates, chemical portioning, and Q-mode factor analysis of metalliferous sediments from the North Fiji Basin. Mar. Geol. 98, 271–295.

Mikhalitsyna, T.I., 2011. The Role of the Permian Lithologic-Sstratigraphic Level in the Formation of Large-Scale Gold Mineralization in the Ayan–Yuryakh Anticlinorium (Southern Flank of the Yana–Kolyma Gold-Bearing Belt). PhD Thesis [in Russian]. DVGI DVO RAN, Magadan.

Mikhalitsyna, T.I., 2014. Lithology and geochemistry of the Upper Permian rocks of the Ayan–Yuryakh anticlinorium (case of the Tikhonya Creek section, Magadan Oblast). Bulletin of the North-East Scientific Center of FEB RAS, No. 4, 17–28.

Mikhalitsyna, T.I., Sotskaya, O.T., 2016. Distribution of rare-earth elements in the ore-bearing strata of the Yana–Kolyma orogenic belt, in: Geology, Geography, Biologic Diversity, and Resources of Northeastern Russia. Proceedings of the Third All-Russian Conference Dedicated to the 105th Birthday of A.P. Vas'kovskii [in Russian]. SVKNII DVO RAN, Magadan, pp. 171–174.

Mirzekhanov, G.S., Mirzekhanova, Z.G., 1991. Stratified Gold–Quartz Mineralization of Carbonaceous-Terrigenous Strata in the Southern Upper Yana Region [in Russian]. DVNTs AN SSSR, Vladivostok.

Muecke, G.K., Pride, C., Sarkar, P., 1979. Rare-earth element geochemistry of regional metamorphic rocks, in: Ahrens, L.H. (Ed.), Origin and Distribution of the Elements. Pergamon Press, Oxford, pp. 449–464.

Nance, W.B., Taylor, S.R., 1976. Rare earth element patterns and crustal evolution — I. Australian post-Archean sedimentary rocks. Geochim. Cosmochim. Acta 40, 1539–1551.

Nekrasov, I.Ya., 1991. Geochemistry, Mineralogy, and Genesis of Gold Deposits [in Russian]. Nauka, Moscow.

Nekrasova, R.A., Nekrasov, I.Ya., 1983. Kularite, an authigenic variety of monazite. Dokl. Akad. Nauk SSR 268 (3), 688–693.

Oreskes, N., Einaudi, M.T., 1990. Origin of rare-earth element enriched hematite breccias at the Olympic Dam Cu–U–Au–Ag deposit, Roxby Downs, South Australia. Econ. Geol. 85 (1), 1–28.

Pluteshko, V.P., Yablokova, S.V., Yanovskii, V.M., 1988. The Natalka deposit, in: Geology of Gold Deposits in the Eastern USSR [in Russian]. TsNIGRI, Moscow, pp. 126–140.

Safonov, Yu.G., 1997. Hydrothermal gold deposits: prevalence, geologic/genetic types, and productivity of ore-forming systems. Geologiya Rudnykh Mestorozhdenii 39 (1), 25–40.

Savchuk, Yu.S., Volkov, A.V., Aristov, V.V., Sidorov, V.A., Lyamin, S.M., 2018. The structure and composition of gold ore shots of the Pavlik deposit. Rudy i Metally, No. 2, 77–85.

Sidorov, A.A., Volkov, A.V., 1998. The peculiarities of coexisting vein and disseminated ores in gold–sulfide deposits. Dokl. Akad. Nauk 362 (4), 533–537.

Sidorov, A.A., Tomson, I.N., 2000. Formation conditions of sulfidized black-shale strata and their metallogenic significance. Tikhookeanskaya Geologiya, No. 1, 37–49.

Sidorov, A.A., Volkov, A.V., 2001. Sources of ore material and formation conditions of gold deposits in northeastern Russia. Dokl. Earth Sci. 377 (2), 143–146.

Sidorov, A.A., Volkov, A.V., 2002. The unique metal potential of ore clusters in the Chukot region. Dokl. Earth Sci. 382 (1), 5–9.

Sidorov, V.A., Goryachev, N.A., Zimenko, E.A., 2003. The Cretaceous volcanic vent of the Vanin stock (Omchak ore cluster), a unique geologic monument, in: Geodynamics, Magmatism, and Minerageny of the Continental Margins of the Northern Pacific [in Russian]. SVKNII DVO RAN, Magadan, Vol. 2, pp. 149–153.

Smagunova, A.N., Karpukova, O.M., 2012. Methods of Mathematical Statistics in Analytical Chemistry [in Russian]. Fenix, Rostov-on-Don.

Sotskaya, O.T., Goryachev, N.A., 2012. Gold and silver microminerals in disseminated sulfide "black-shale" ores (northeastern Russia), in: Geology and Mineral Resources of Northeastern Russia [in Russian]. Izd. Dom SVFU, Yakutsk, Vol. 2, pp. 173–177.

Sotskaya, O.T., Goryachev, N.A., Goryacheva, E.M., Nikitenko, E.M., 2012. Micromineralogy of "black shale" disseminated-sulphide gold ore deposit of the Ayan-Yuryakh anticlinorium (North-East of Russia). J. Earth Sci. Eng. 2 (12), 744–753.

Sotskaya, O.T., Goryachev, N.A., Mayorova, T.P., 2014. Micromineralogy of the Chudnoe deposit (Polar Ural), in: Precious Metals, Rare and Radioactive Elements in Ore-Forming Systems. Proceeding of the Russian Scientific Conference with International Participation Dedicated to the 120th Anniversary of the birth of Corresponding member of the USSR Academy of Sciences, Professor Felix Shakhov [in Russian]. INGG SO RAN, Novosibirsk, pp. 664–668. http://shakhov.igm.nsc.ru/pdf/Shakhov120-p660_663.pdf.

Struzhkov, S.F., Natalenko, M.V., Chekvaidze, V.B., Isakovich, I.Z., Golubev, S.Yu., Danil'chenko, V.A., Obushkov, A.V., Zaitseva, M.A., Kryazhev, S.G., 2006. Multivariate model of the Natalka gold deposit. Rudy i Metally, No. 3, 34–44.

Tarasova, Yu.I., Sotskaya, O.T., Skuzovatov, S.Yu., Vanin, V.A., Kulikova, Z.I., Budyak, A.E., 2016. Mineralogical and geochemical evidence for multi-stage formation of the Chertovo Koryto deposit. Geodyn. Tectonophys. 7 (4), 663–677.

Taylor, S.R., McLennan, S.M., 1985. The Continental Crust: Its Composition and Evolution. Blackwell, Oxford.

Tomich, S.A., 1986. An outline of the economic geology of Kalgoorlie, Western Australia. Trans. Geol. Soc. S. Afr. 89 (1), 35–55.

Tyukova, E.E., Voroshin, S.V., 2003. The temperature of formation of sulfide parageneses in the Upper Kolyma region according to the data on sulfur isotope ratios, in: Geodynamics, Magmatism, and Minerageny of the Continental Margins of the Northern Pacific [in Russian]. SVKNII DVO RAN, Magadan, Vol. 2, pp. 211–213.

Tyukova, E.E., Mikhalitsyna, T.I., Vikent'eva, O.V., 2007. REE mineralization of the Natalka gold–quartz deposit (Magadan Region), in: Geochemistry and Formation of Ores of Radioactive, Precious, and Rare Metals during Endogenous and Exogenous Processes [in Russian]. BNTs SO RAN, Ulan-Ude, Part 1, pp. 168–171.

Vedernikov, I.L., 2009. Distribution of organic carbon in the Permian gold-bearing strata of the Ayan–Yuryakh anticlinorium, in: Abstracts of the Academician K.V. Simakov Memorial All-Russian Scientific Conference [in Russian]. SVNTs DVO RAN, Magadan, pp. 43–44.

Volkov, A.V., Sidorov, A.A., Murashov, K.Yu., Sidorova, N.V., 2016. New data on ore geochemistry of the Rodionovskoe gold–quartz deposit, Northeast Russia. Russ. J. Pacific Geol. 10 (5), 386–394.

Voroshin, S.V., Sidorov, V.A., Tyukova, E.E., Pristavko, V.A., Mel'nik, V.G., 1995. Geology, geochemistry, mineralogy, and platinum potential of the Natalka gold deposit, in: Platinum of Russia [in Russian]. Geoinformmark, Moscow, Vol. 2, Book 2, pp. 161–176.

Voroshin, S.V., Tyukova, E.E., Chinenov, V.A., 2000. The isotopic composition of carbon and oxygen in the host rocks and ores of the Natalka deposit. Kolyma, No. 2, 58–65.

Yapaskurt, O.V., 1999. Premetamorphic Alterations of Sedimentary Rocks in the Stratisphere. Processes and Factors [in Russian]. GEOS, Moscow.

Yudovich, Ya.E., Ketris, M.P., 2000. The Fundamentals of Lithochemistry [in Russian]. Nauka, St. Petersburg.

Zakharevich, K.V., Kotov, N.V., Vaganov, P.A., Kol'tsov, A.B., 1987. Gold–Silver Ore Metasomatites in Black-Shale Strata [in Russian]. LGU, Leningrad.

Editorial responsibility: A.S. Borisenko